graphene

the mother of all carbon nanostructures

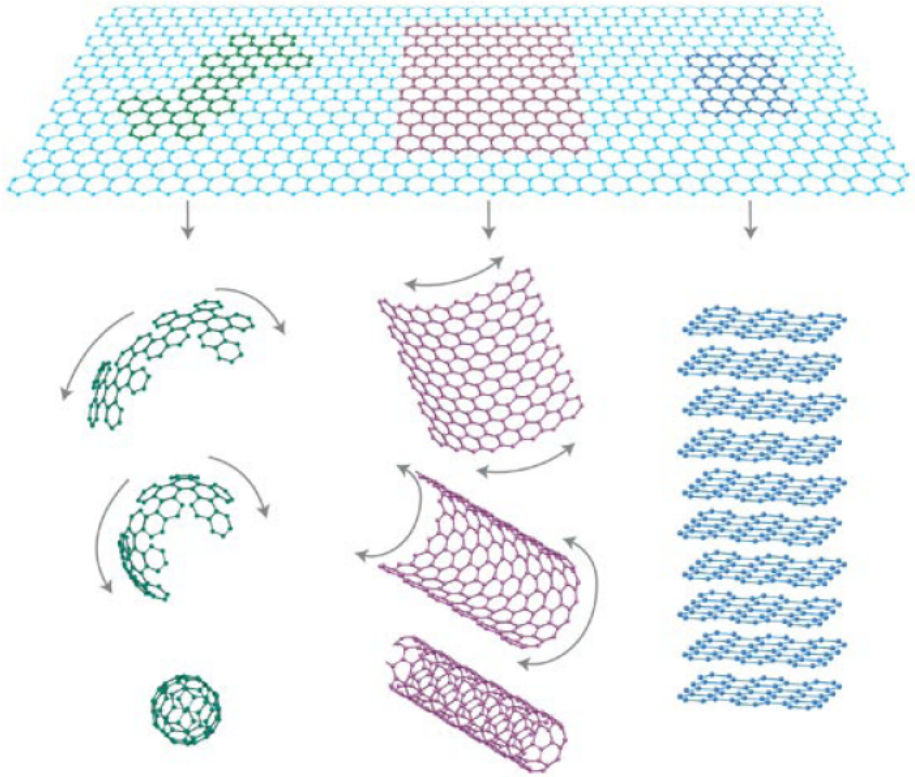

CNTs discover

A paper by Oberlin, Endo, and Koyama published in **1976** clearly showed hollow carbon fibers with nanometer-scale diameters using a vapor-growth technique (Oberlin, A.; M. Endo, and T. Koyama, J. Cryst. Growth (March 1976). *Filamentous growth of carbon through benzene decomposition*. **32**. pp. 335–349.)

Iijima, Sumio (**1991**). "Helical microtubules of graphitic carbon". *Nature* **354**: 56–58.

Fullerenes

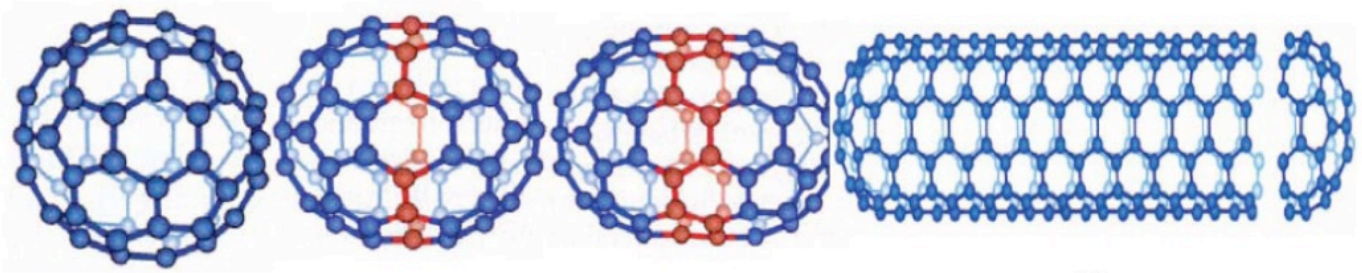

nanotubes

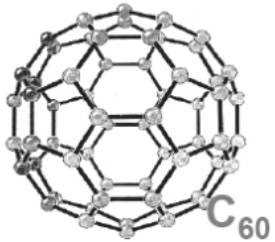

Fullerenes

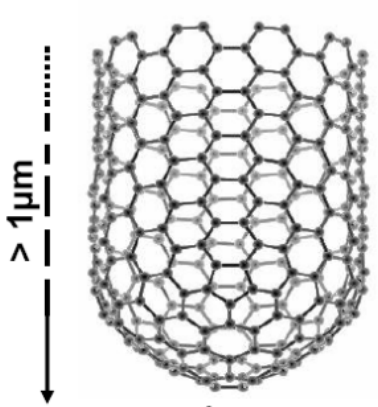

Nanotubes

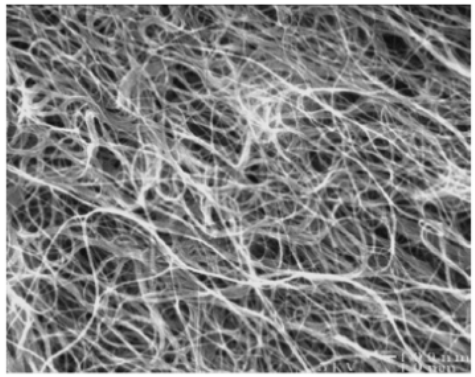

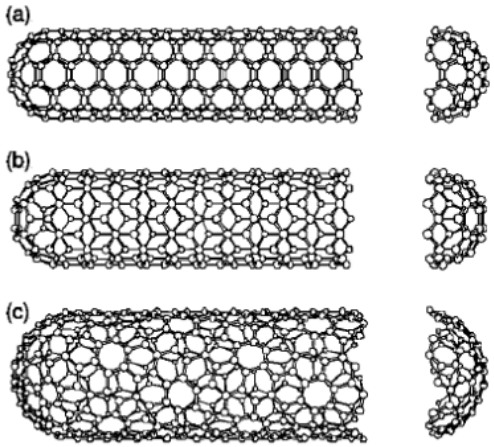

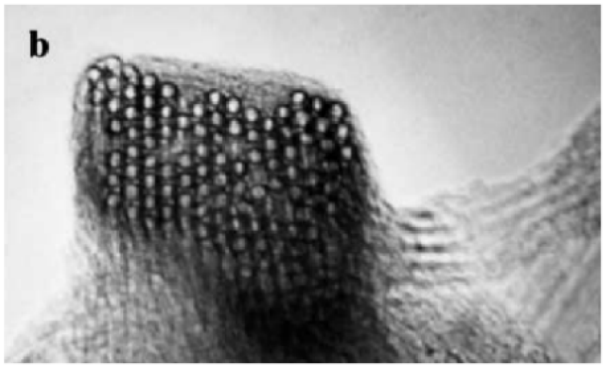

structure

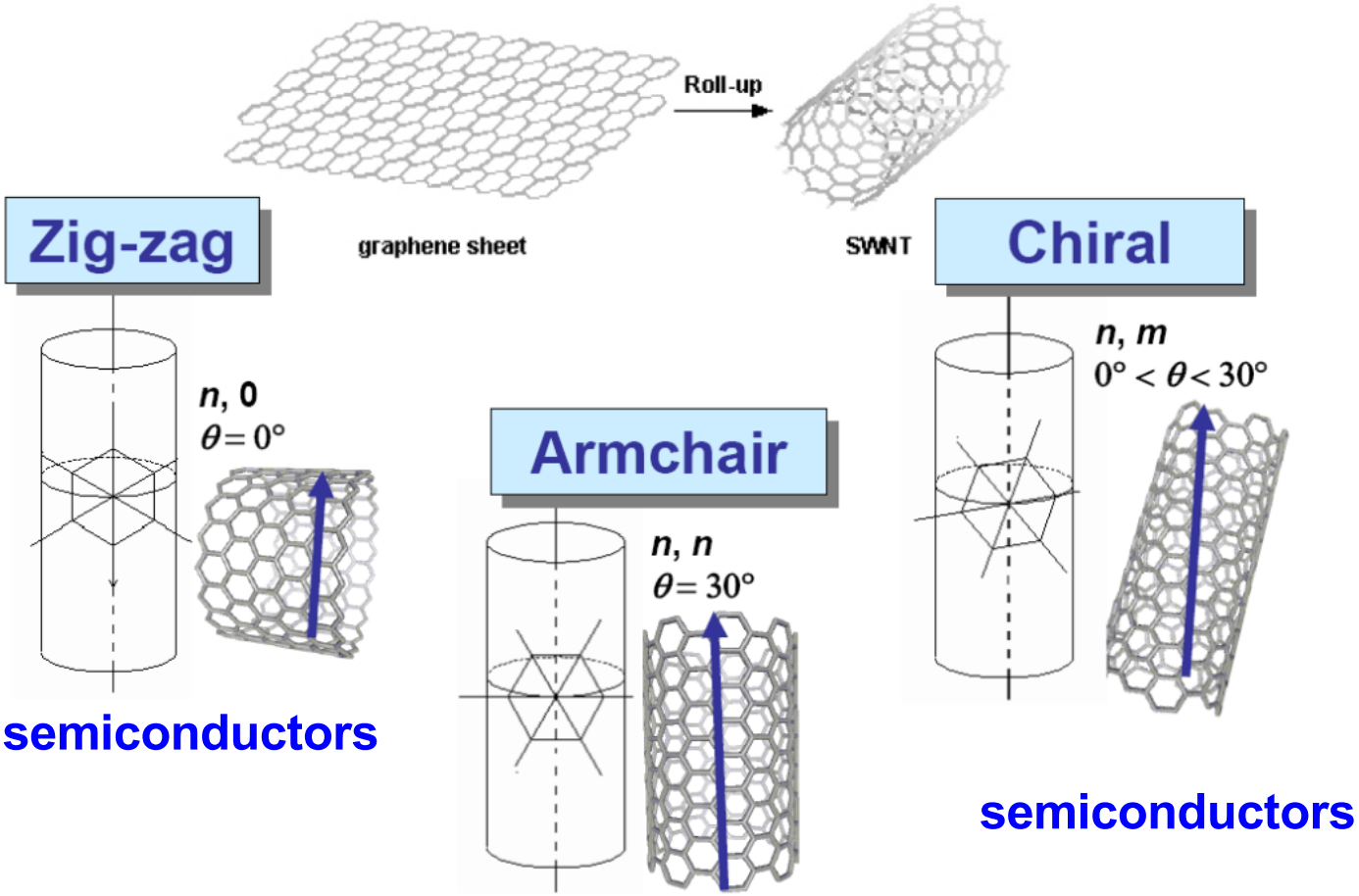
Roll-up
graphene sheet
SWNT
Zig-zag
n, 0
θ = 0°
semiconductors
Armchair
n, n
θ = 30°
metallic character
Chiral
n, m
0° < θ < 30°
semiconductors

Structure

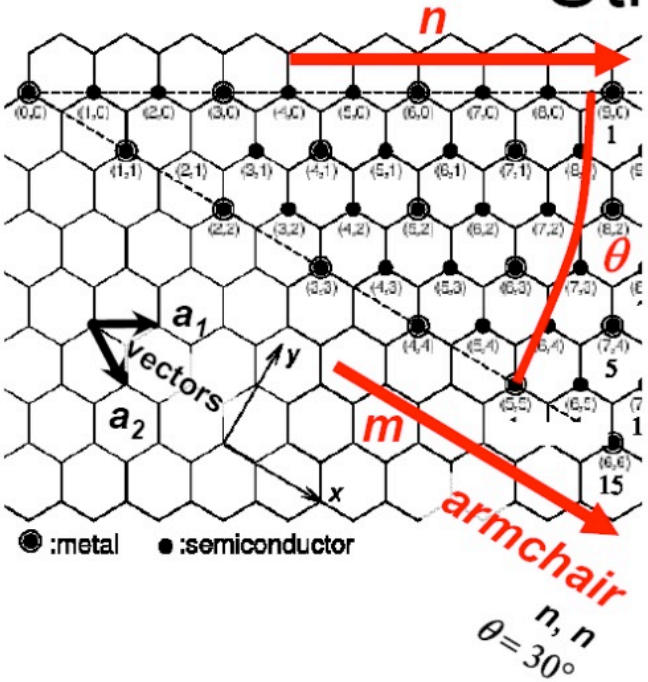

roll-up vector

$$C_h = n\hat{\mathbf{a}}_1 + m\hat{\mathbf{a}}_2$$

wrapping angle

$$\theta = \tan^{-1}[\sqrt{3}n/(2m+n)]$$

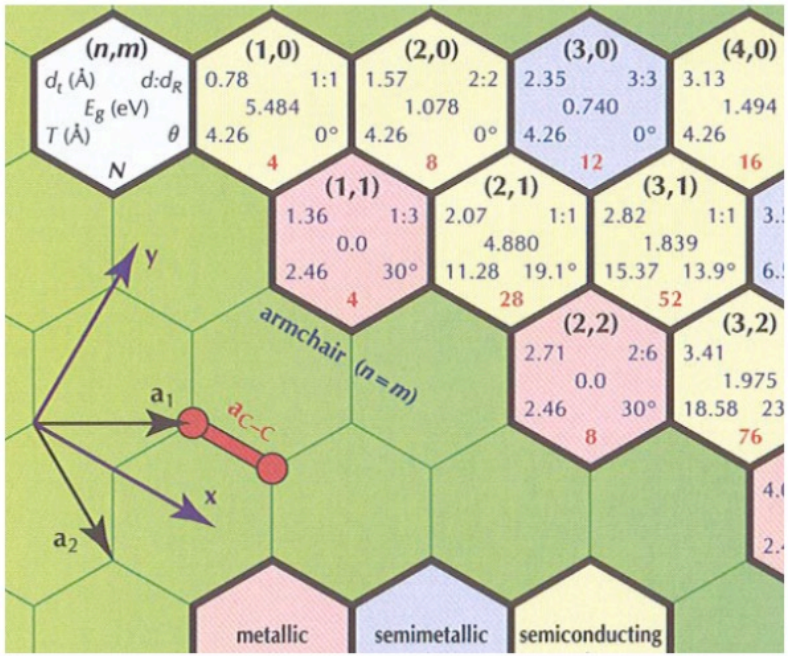

nanotube (*n*,*m*)

armchair SWCNT posses a **metallic character**
the other behave as **semiconductors**

CNTs structures

The integers *n* and *m* denote the number of unit vectors along two directions in the honeycomb crystal lattice of graphene.
If *m*=0, the nanotubes are called "zigzag".
If *n*=*m*, the nanotubes are called "armchair".
Otherwise, they are called "chiral".

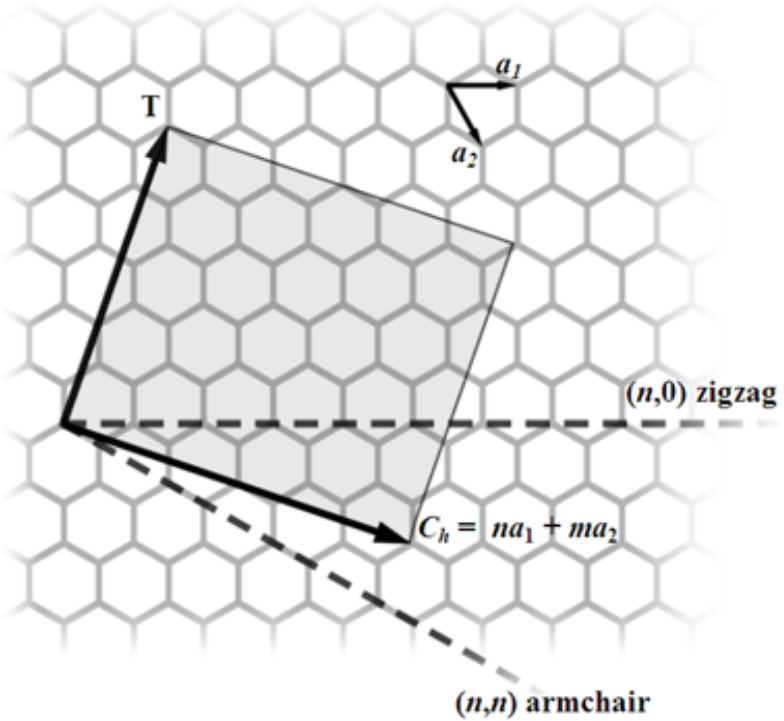

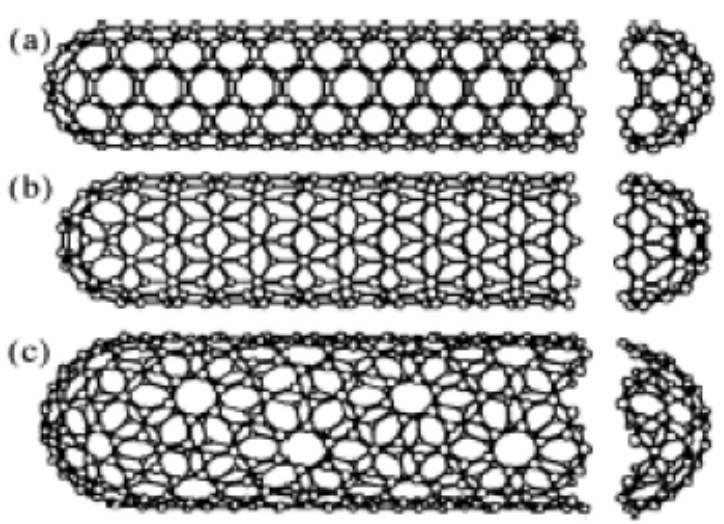

Some SWNTs with different chiralities. The difference in structure is easily shown at the open end of the tubes. a) armchair structure b) zigzag structure c) chiral structure

CNTs properties

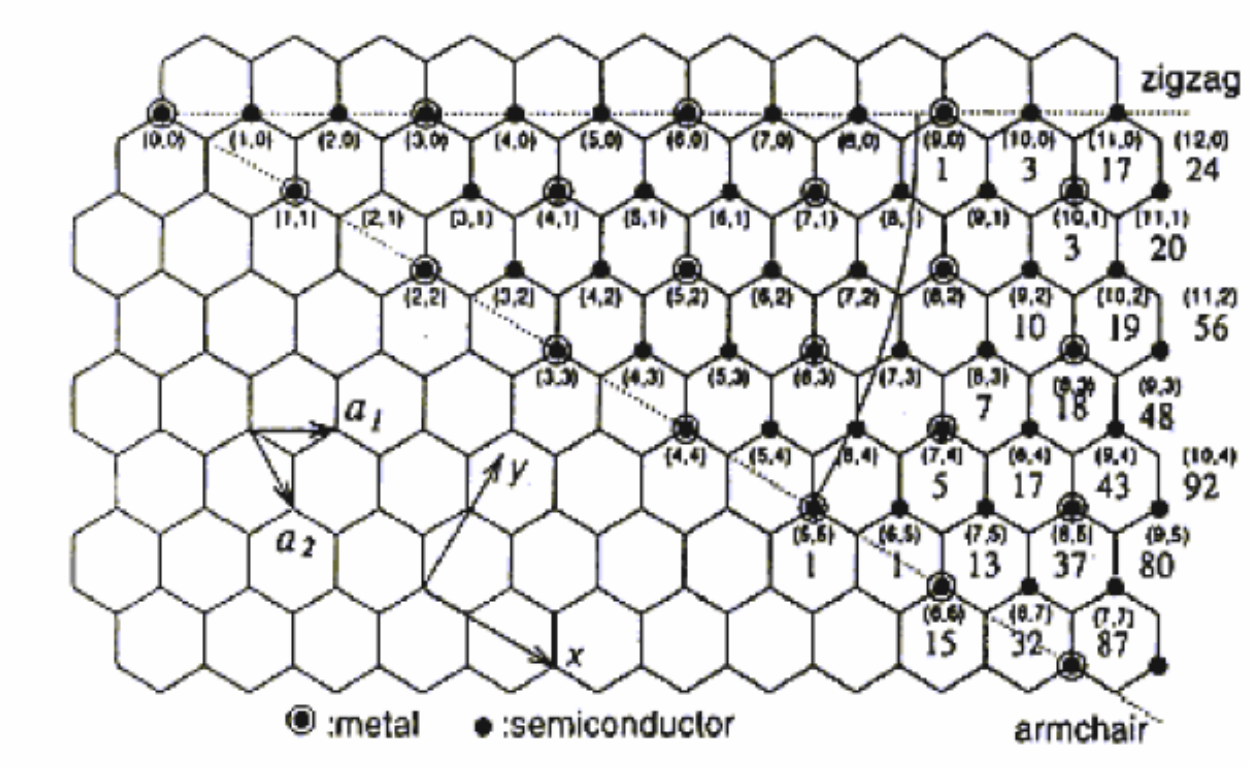

Figure 1-3: All possible structures of SWNTs can be formed from chiral vectors lying in the range given by this figure. (n,m) with n,m integer and m<=n or θ <30°.[5]

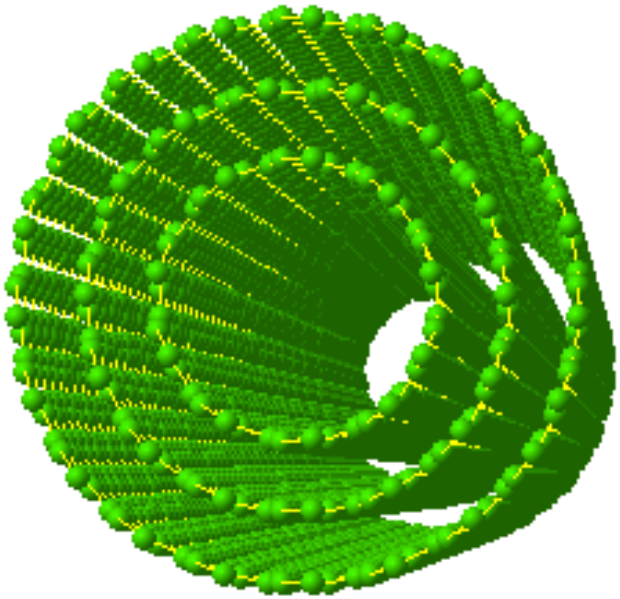

Multiwall nanotubes

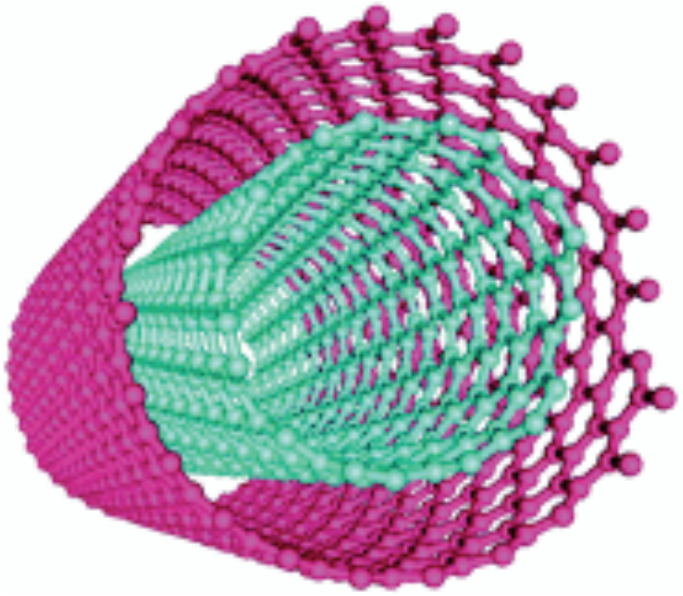

Double wall nanotubes

CNTs structures

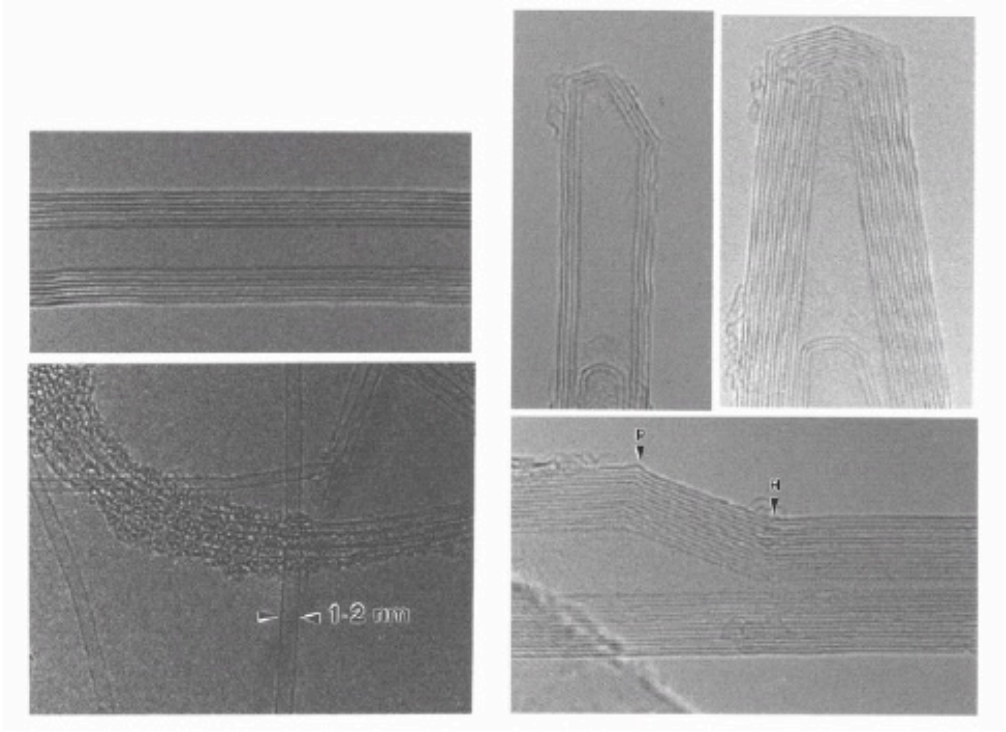

Figure 1-4: Different structures of MWNTs. Top-left: cross-section of a MWNT the different walls are obvious, they are separated by 0.34nm. Rotation around the symmetry axis gives us the MWNT. Top-right: Symmetrical or non-symmetrical cone shaped end caps of MWNTs. Bottom-left: A SWNT with a diameter of 1,2nm and a bundle of SWNTs covered with amorphous carbon. Bottom-right: A MWNT with defects. In point P a pentagon defect and in point H a heptagon defect.[6]

CNTs structures

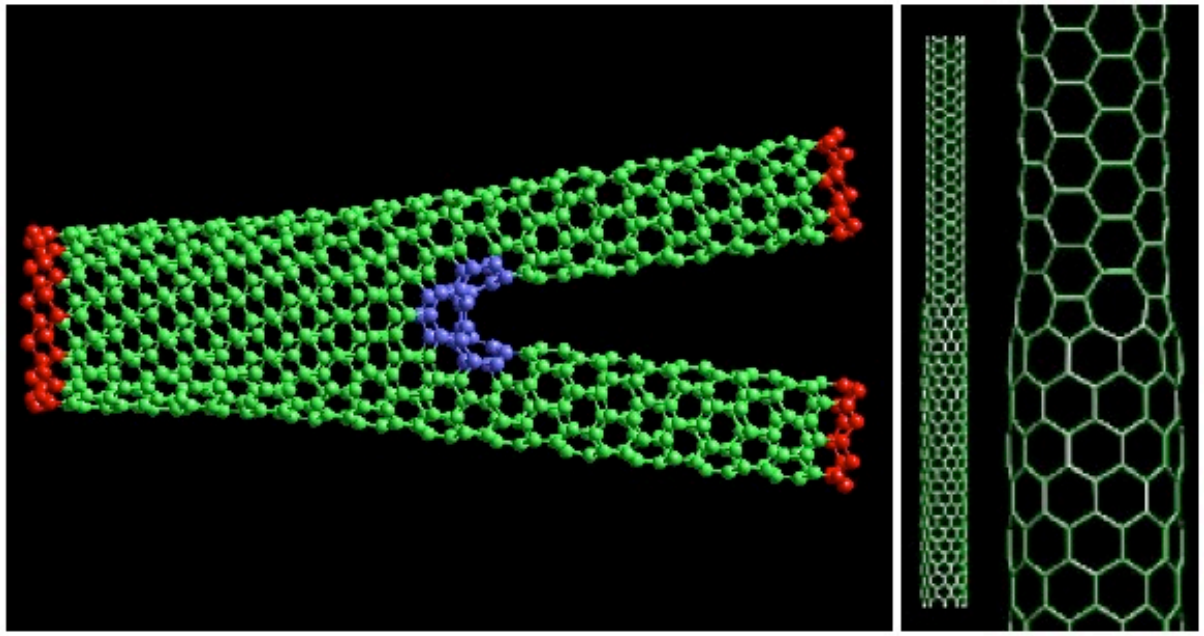

Figure 1-5: Left: A Y-branch, the defects are marked in blue. Right: A transition from a metallic to a semi-conducting SWNT. The change is made by insertion of pentagons and heptagons.

CNTs properties

SWNTs with different chiral vectors have dissimilar properties such as optical activity, mechanical, strength and electrical conductivity.

CNTs are 100 times stronger than steel

Comparison of Mechanical Properties

Material	Young's Modulus(1) (GPa)	Tensile Strength (GPa)	Elongation at Break (%)
SWNT	~1 (from 1 to 5)	13-53[E]	16
Armchair SWNT	0.94[T]	126.2[T]	23.1
Zigzag SWNT	0.94[T]	94.5[T]	15.6-17.5
Chiral SWNT	0.92		
MWNT	0.8-0.9[E]	150	
Stainless Steel	~0.2	~0.65-1	15-50
Kevlar	~0.15	~3.5	~2
Kevlar[T]	0.25	29.6	

1. misura della durezza di un materiale elastico

(The tangent modulus of the initial, linear portion of a stress-strain curve is called *Young's modulus)*

around $1500 per gram as of 2000
~$50–100 per gram as of 2007

Kevlar

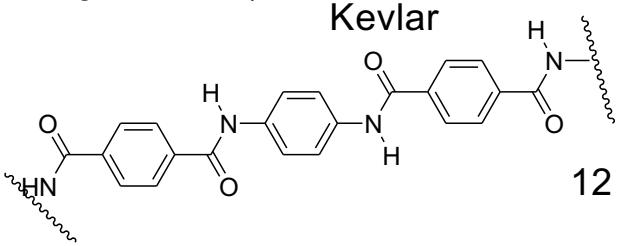

Potential applications of CNTs

Electronics

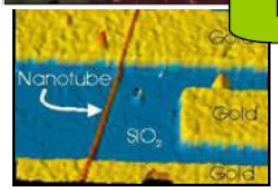

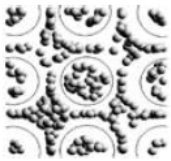

Gas storage

Composite materials

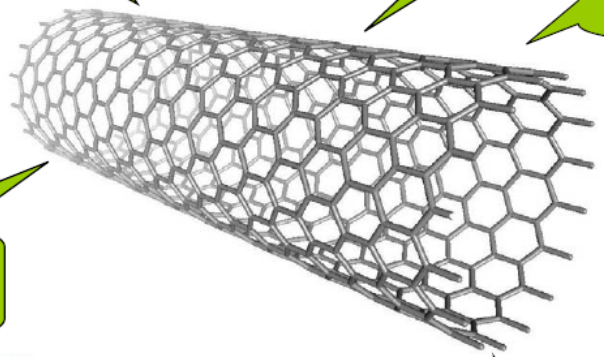

Bio-medicine

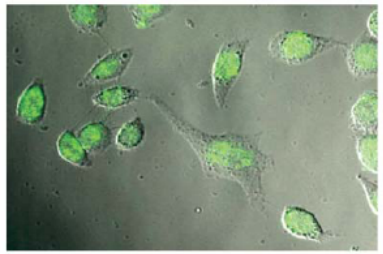

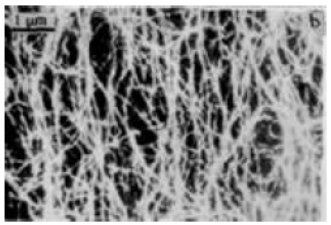

Nano-fibers

Scanning probes

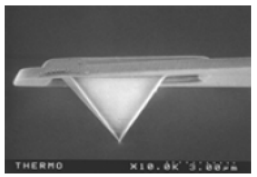

Synthesis: arc discharge

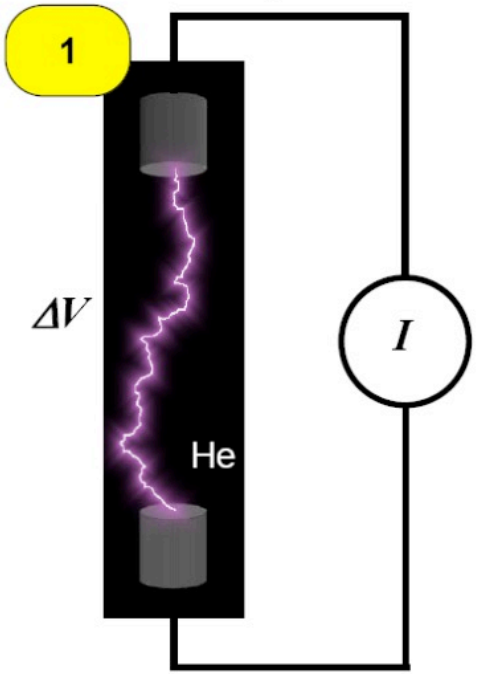

T = 3000 – 4000 °C (graphite mp)

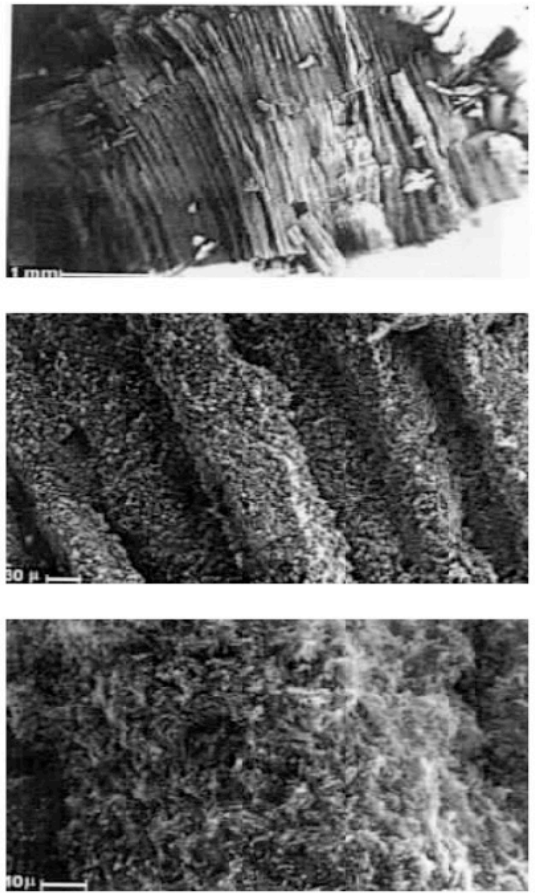

Laser Ablation

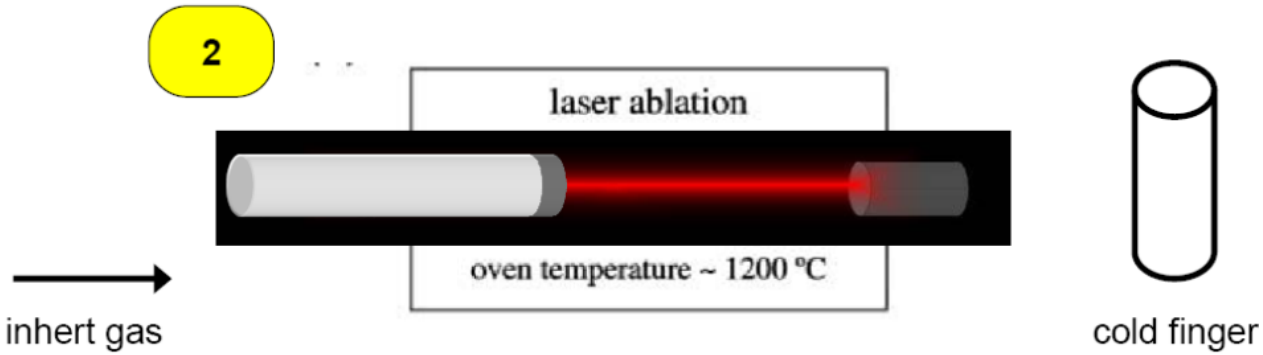

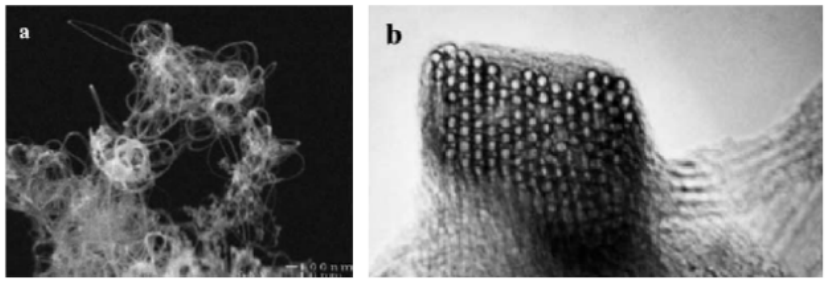

purification

Oxidation
- acid solution
- air at high T

Separation
- surfactants
- chromatography

Annealing

10.5 %

1 %

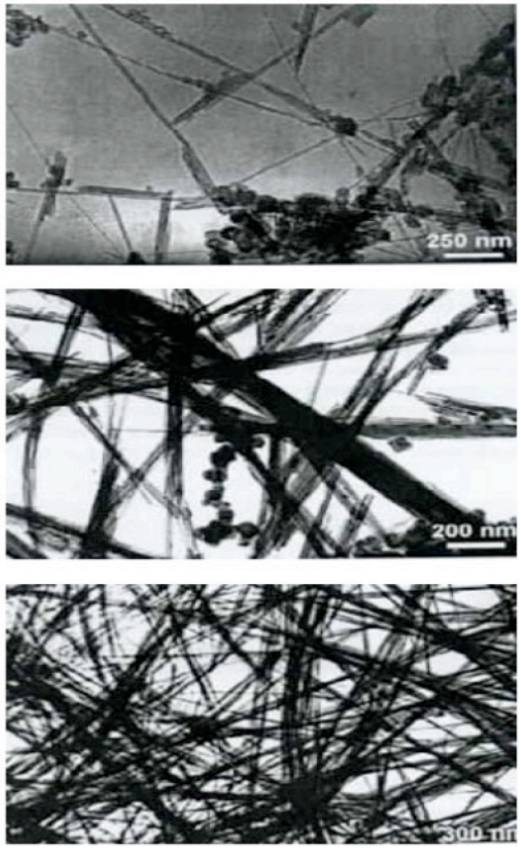

C. Furtado et al., *J. Am. Chem. Soc.* **2004**, *126*, 6095-6105

R. C. Haddon et al., *Mrs Bulletin* **2004**, *29*, 252-259.

Covalent Functionalization of CNTs

SCHEME 2. Oxidation of Carbon Nanotubes

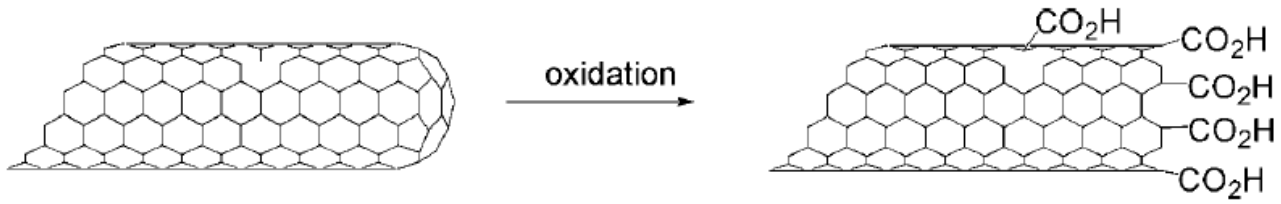

SCHEME 3. Amidation Reaction of Oxidized Carbon Nanotubes

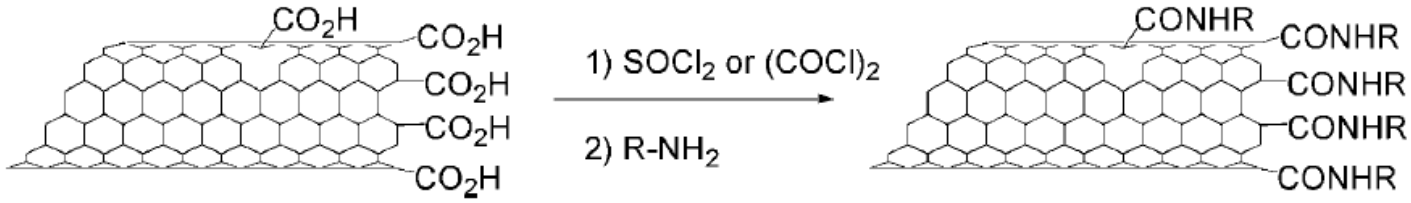

SCHEME 4. Functionalization of Carbon Nanotubes Using Addition Reactions (X = Functional Groups)

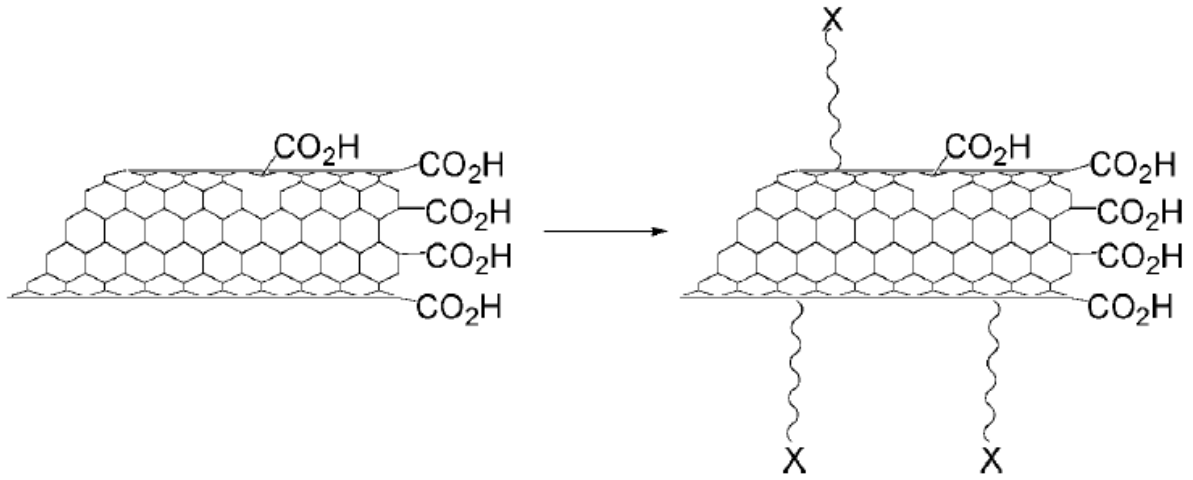

Carbon Nanotubes in Drug Design and Discovery *Prato et al.* **ACCOUNTS OF CHEMICAL RESEARCH** 2008, 41, 60-68.

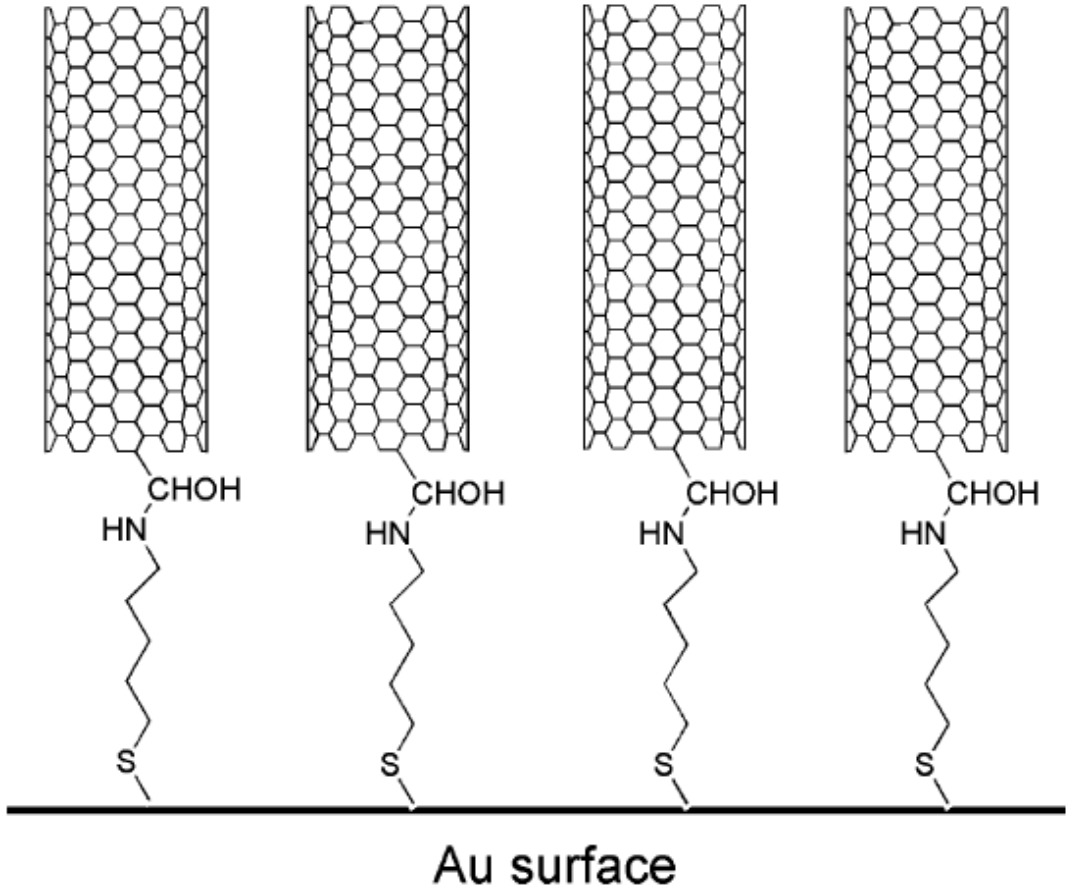

Figure 18. Controlled deposition of oxidized nanotubes onto gold surfaces by using aminothiols as chemical tethers.

D. Tasis, N. Tagmatarchis, A. Bianco, M. Prato Chem. Rev. **2006,** 106, 1105-1136

SCHEME 5. Insertion inside Carbon Nanotubes

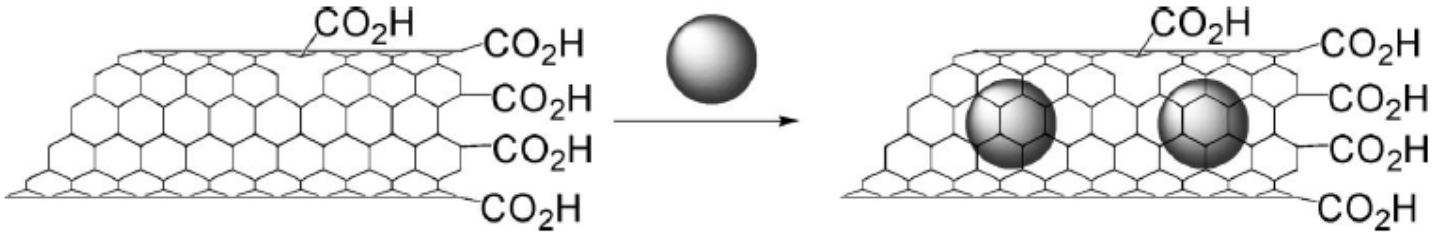

fullerenes, porphyrins, and metals, have indeed been included
in the internal space of CNT, mostly due to hydrophobic interactions

TABLE 1. Molecular Structures of the Carbon Nanotube Conjugated with Different Therapeutic Agents

Compounds	Bioassays
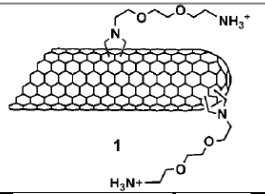 1	Cell internalization[24, 26, 27] Intracellular trafficking[24, 27] Cell viability[26] Plasmid DNA delivery[26, 32]
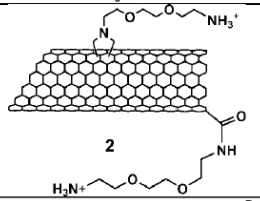 2	Precursor for the preparation of CNT **4** and **5**
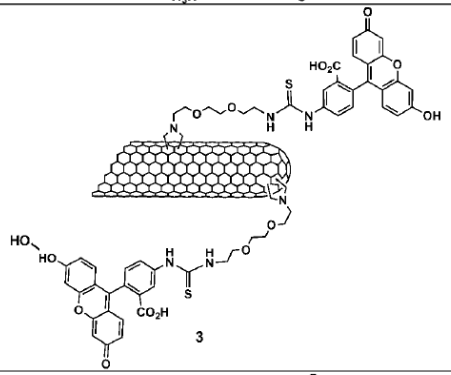 3	Cell internalization[23-25] Intracellular trafficking[23-25] Cell viability[23-25]
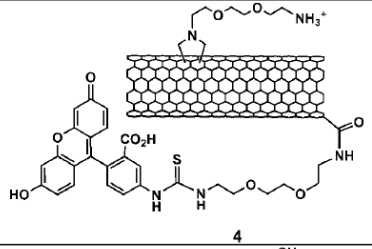 4	Cell internalization[24]
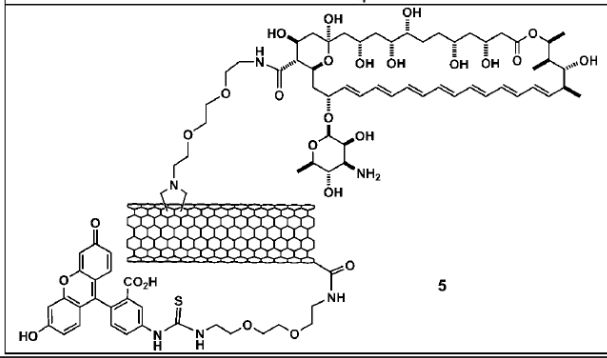 5	Cell internalization[22, 24] Cell viability[22]

fluorescein

fluorescein

amphotericin B and fluorescein

TABLE 1. Continued

Compounds	Bioassays
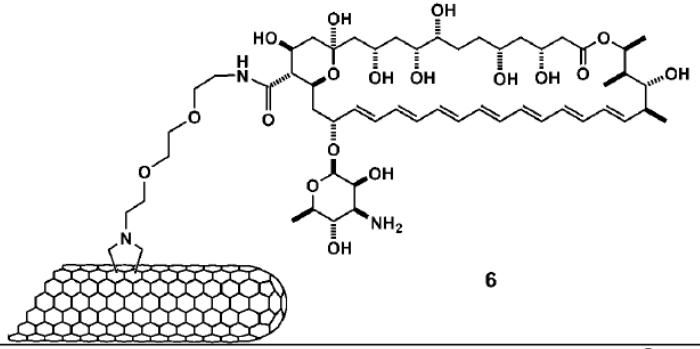 6	Antibiotic delivery[22]
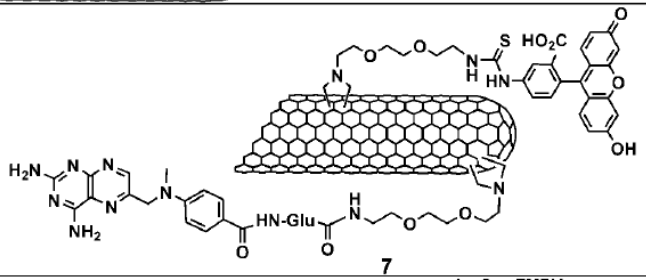 7	Cell internalization[36] Cell viability[36] Anticancer delivery[36]
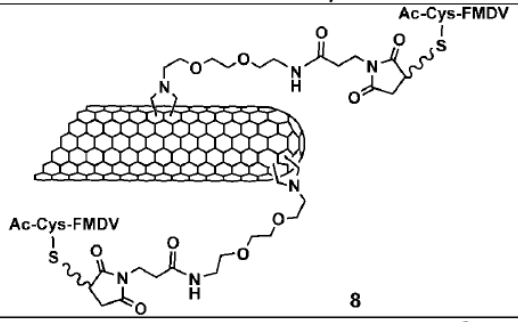 8	Immunogenic activity[41, 42] (FMDV peptide corresponds to the 141-159 region of the viral envelope protein VP1 from foot-and-mouth disease virus)
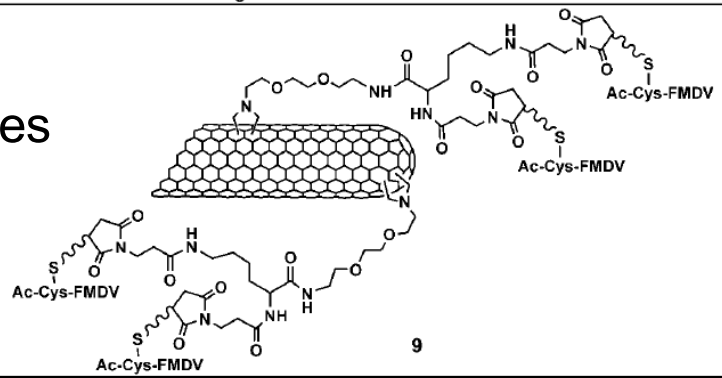 9	Immunogenic activity[42] (FMDV peptide corresponds to the 141-159 region of the viral envelope protein VP1 from foot-and-mouth disease virus)

anticancer agent
methotrexate

immunogenic peptides

immunogenic peptides

Noncovalent Functionalization of CNTs

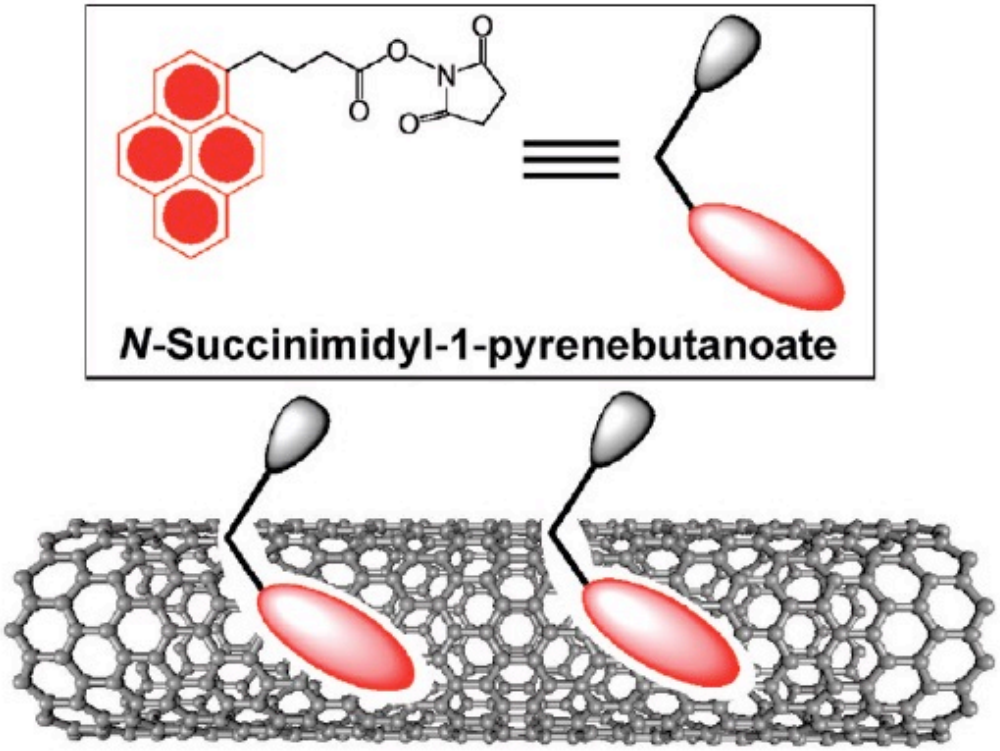

FIGURE 2. Schematic representation of *N*-succinimidyl-1-pyrenebutanoate-decorated SWNT.

Noncovalent Functionalization of SWNTs *Zhao and Stoddart* **ACCOUNTS OF CHEMICAL RESEARCH, 2009, 42,** 1161-1171.

modifica delle proprietà di CNTs

modulation of the electrical conductance

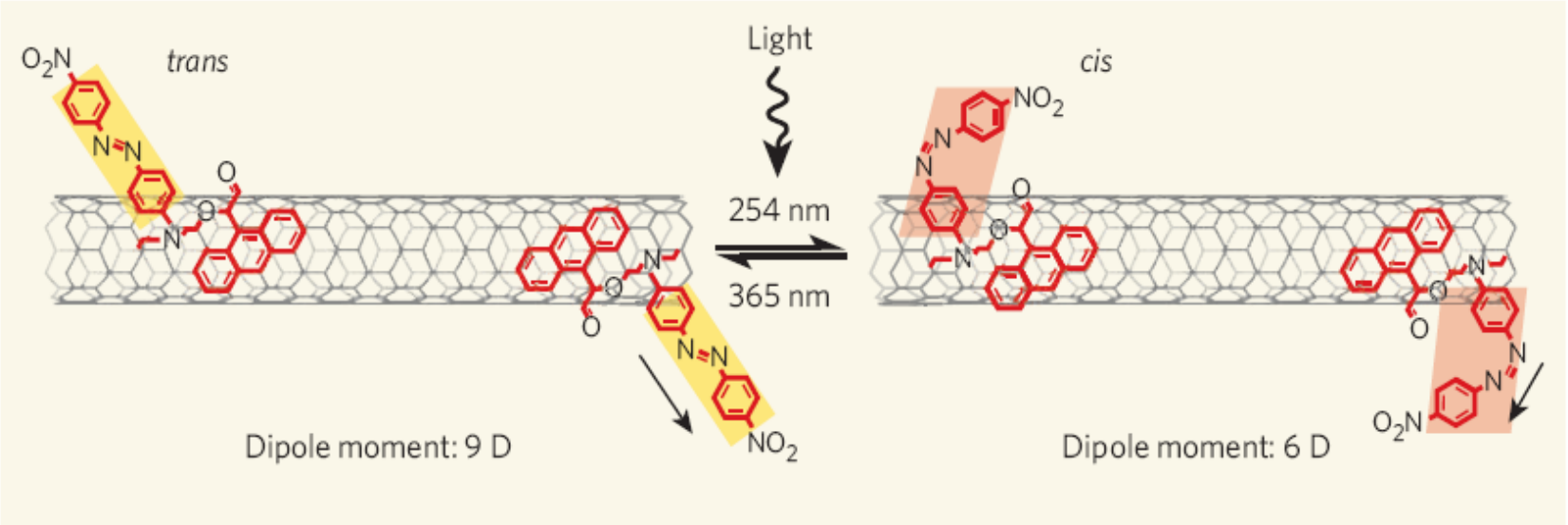

Figure 1 | Light bending and stretching. Simmons *et al.*[1] make the conductivity of carbon nanotubes responsive to light by adding molecules of the azo-based Disperse Red 1 dye to the nanotube walls. These dye molecules undergo photoisomerization, with their molecular conformation shifting around their central nitrogen double bond: from the *trans* to the *cis* form under ultraviolet light of wavelength 254 nm, and back again under blue light of 365 nm. The changes cause significant, reversible shifts in the molecules' electrical dipole moments (unit: debye, D; arrows indicate direction), and thus in the electrical conductance of a nanotube transistor as a whole.

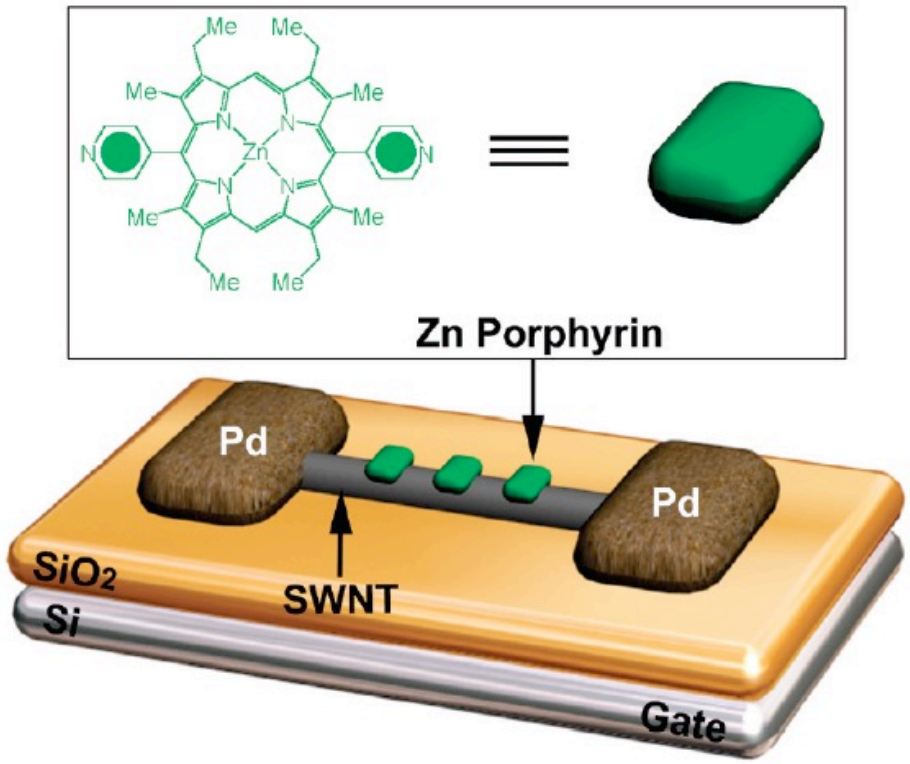

FIGURE 3. Schematic representation of the zinc porphyrin-coated SWNT/FET device employed for transistor measurements.

to detect photoinduced electron transfer between ZnPorphyrin and CNT

The SWNTs act as the electron donors, and the porphyrin molecules act as the electron acceptors. The photoresponse of the zinc porphyrin-coated SWNT/FET was investigated by its illumination with a light-emitting diode (LED) centered at 420 nm,

Hecht, D. S.; Ramirez, R. J. A.; Briman, M.; Artukovic, E.; Chichak, K. S.; Stoddart, J. F.; Gru¨ ner, G. Bioinspired detection of light using a porphyrin-sensitized singlewall nanotube field effect transistor. *Nano Lett.* 2006, *6*, 2031–2036.

sensori

serve as chemical sensors to detect nonfluorescent organic molecules selectively, on the basis of their molecular recognition by the cyclodextrin torus.

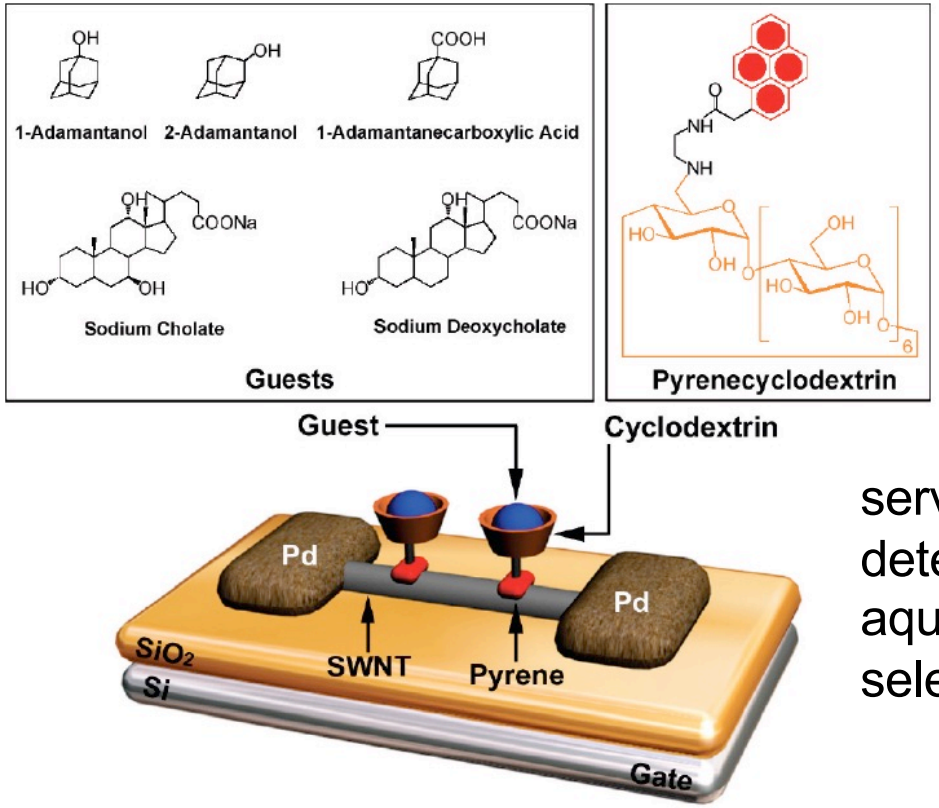

1-adamantanol > 2-adamantanol> 1-adamantanecarboxylic acid > sodium deoxycholate > sodium cholate.

serve as chemical sensors to detect organic molecules in aqueous solution, not only selectively but also quantitatively.

FIGURE 5. Schematic representation of the pyrenecyclodextrin-decorated SWNT/FET device showing how pyrenecyclodextrin-decorated SWNTs interact with guest molecules when they are being sensed in a FET device. The five guest molecules employed were 1-adamantanol, 2-adamantanol, 1-adamantanecarboxylic acid, sodium cholate, and sodium deoxycholate.

Satisfyingly, the magnitude of the transistor characteristic movements in the pyrenecyclodextrin-SWNT/FET devices in the presence of the organic molecules depends linearly upon the magnitudes of the complex formation constants (*K*S) exhibited by the pyrenecyclodextrin derivative with these molecules.

Zhao, Y.-L.; Hu, L.; Stoddart, J. F.; Gru¨ ner, G. Pyrenecyclodextrin-decorated singlewalled carbon nanotube field-effect transistors as chemical sensors. *Adv. Mater.* 2008, *20*, 1910–1915.

Hybrid CNTs-NPs materials

- Formation of metal nanoparticles directly on the carbon nanotube surface
- Connecting metal nanoparticles and CNTs

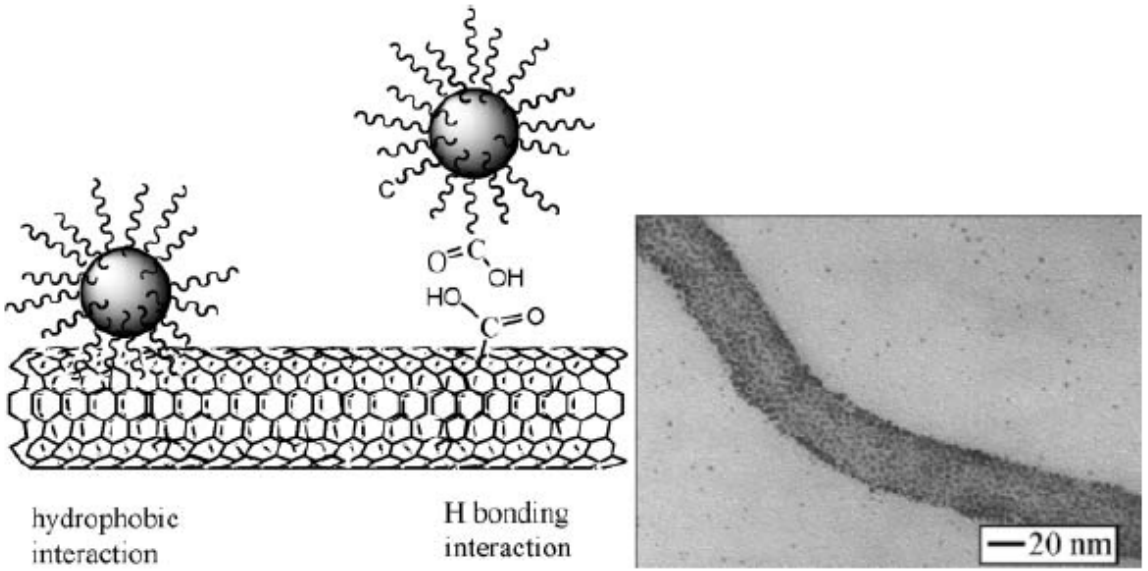

Fig. 14 Schematic illustrations of the assembly of mixed-monolayer capped NPs on oxidized CNTs and a characteristic TEM image of the resulting derivative (reproduced with permission from ref. 57).

"Decorating carbon nanotubes with metal or semiconductor nanoparticles".

V. Georgakilas, D. Gournis, V. Tzitzios, L. Pasquato, D. M. Guldi, M. Prato, *J. Mater. Chem.* **2007**, *17*, 2679-2694.

L. Han, W. Wu, F. L. Kirk, J. Luo, M. M. Maye, N. N. Kariuki, Y. Lin, C. Wang and C. J. Zhong, *Langmuir*, **2004**, *20*, 6019.

Connecting metal nanoparticles and CNTs

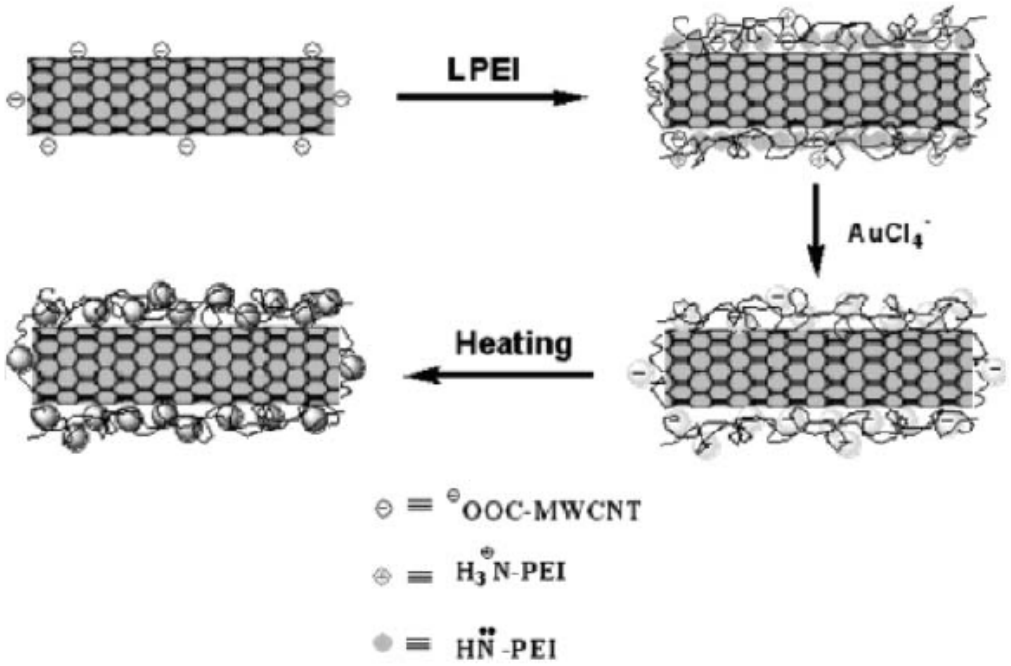

Fig. 22 Schematic illustration of the experimental procedure in which PEI possibly interacts with acid-functionalized MWNTs through electrostatic interaction and physisorption processes (reproduced with permission from ref. 73)

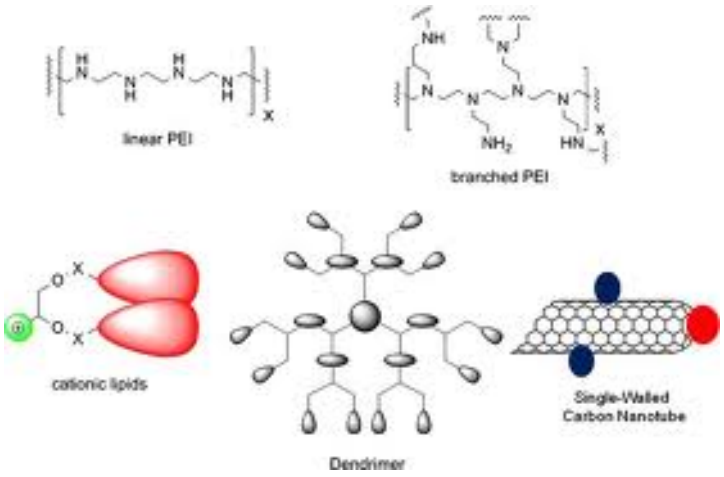

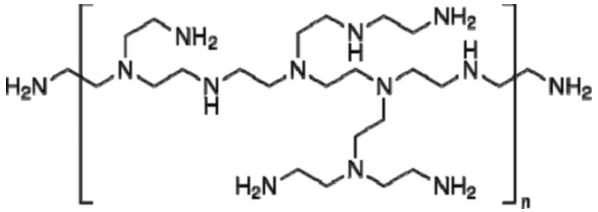

PEI = polyethyleneimine

X. Hu, T. Wang, X. Qu and S. Dong, J. Phys. Chem. B, 2006, 110, 853.

Covalent Chemistry

Addition of dichlorocarbene

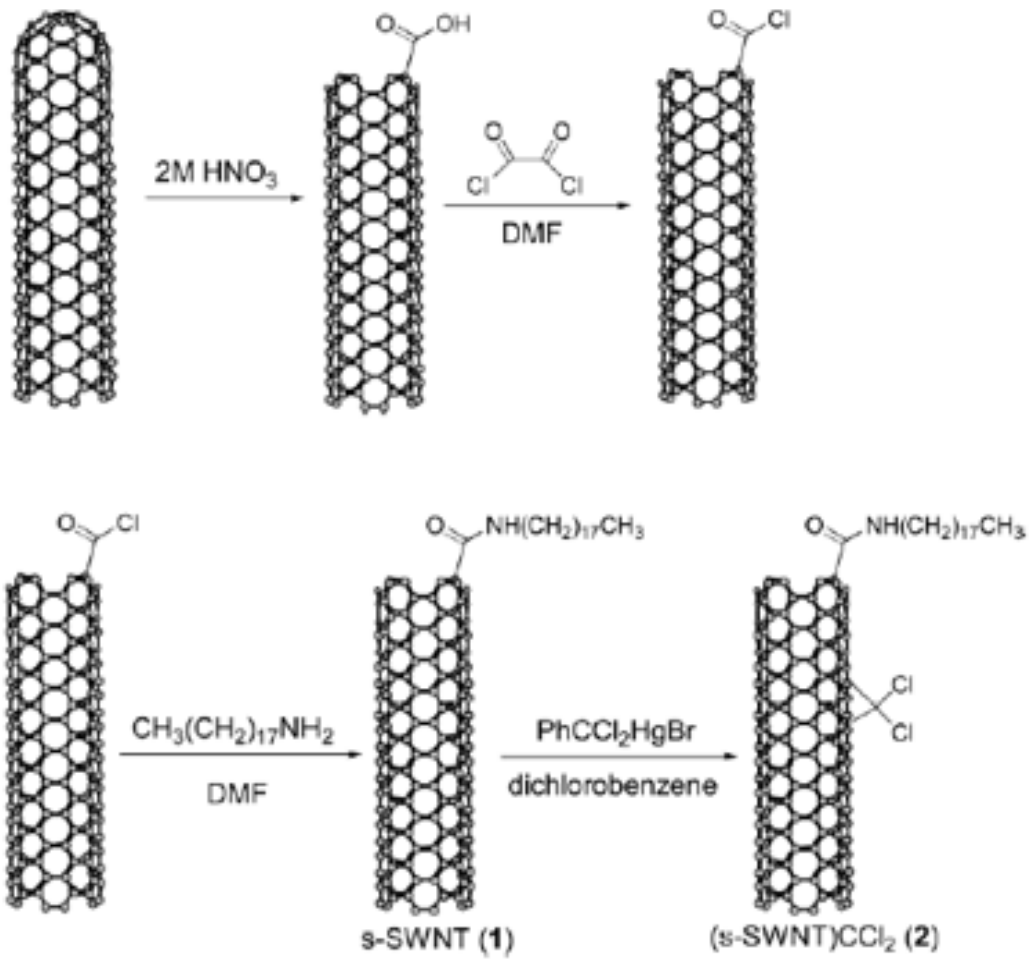

JACS 2003, 125, 14893

Addition of carbenes and nitrenes

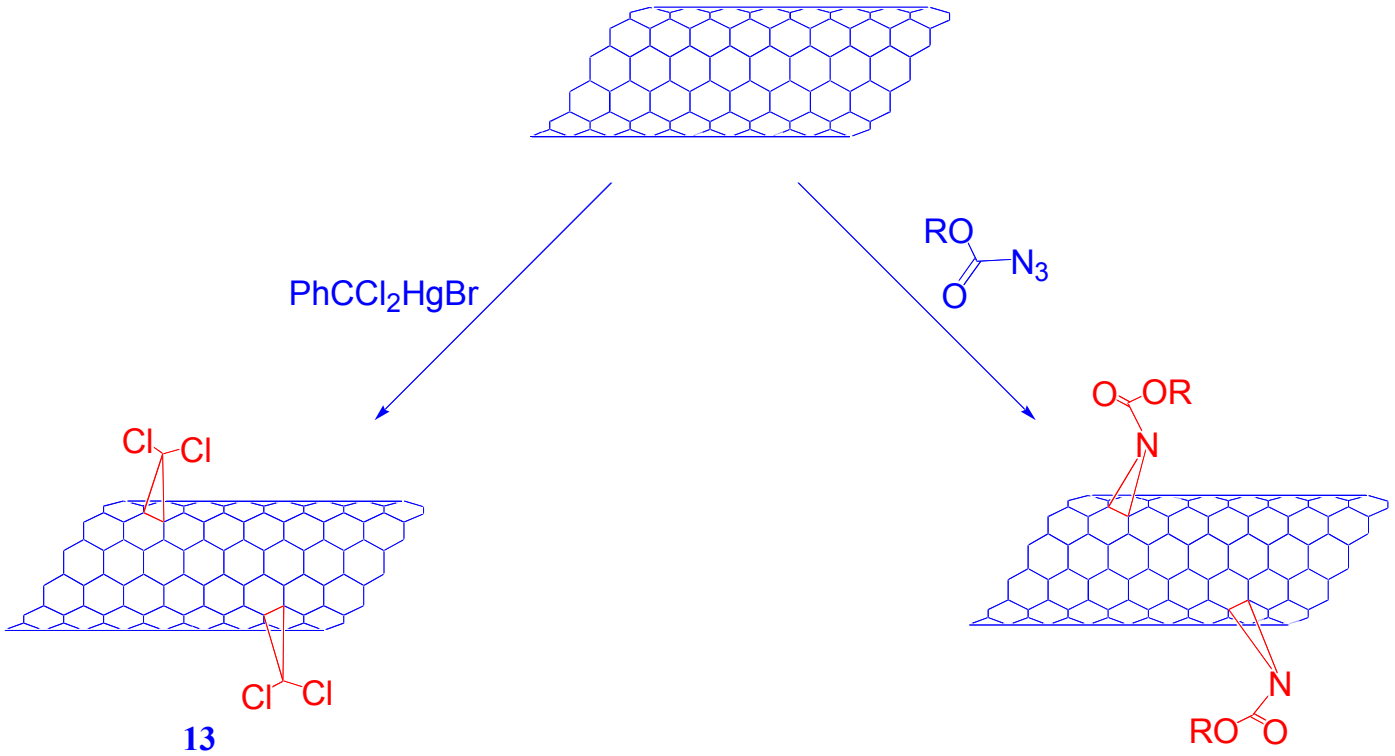

Science 2003 p1501, JACS 2003 p14893

14 R = Ethyl
15 R = *tert*-Butyl
16 R =
17 R =
18 R =
19 R =
20 R =
21 R =
22 R =
23 R =

24 R =
25 R =

26 R =
27 R =
28 R =

AC 2001 p4002, JACS 2003 p8566

Cycloadditions

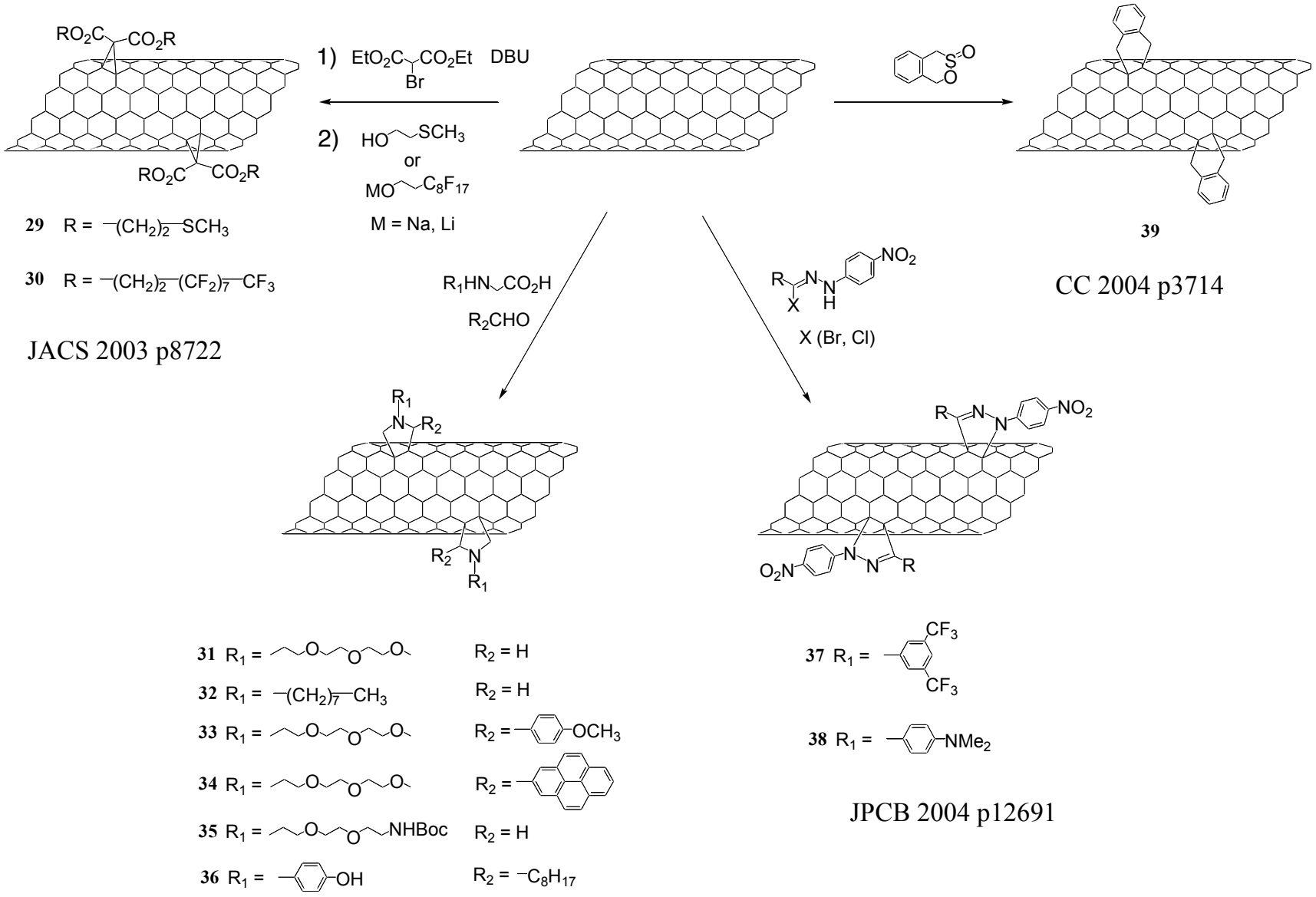

JACS 2002 p760, CC 2002 p3050, JACS 2003 p16015

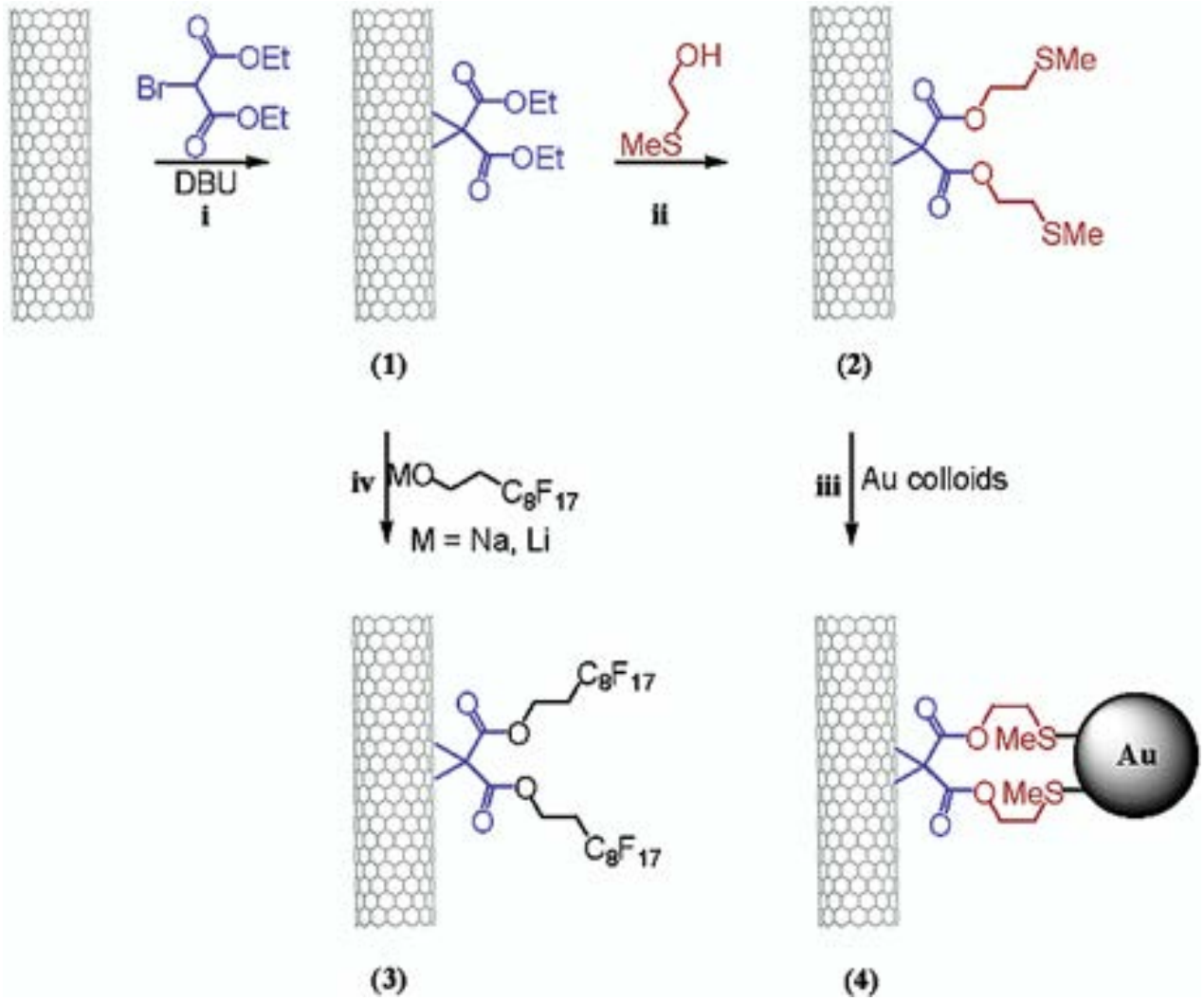

J. Am. Chem. Soc., 125 (29), 8722 -8723, 2003 33

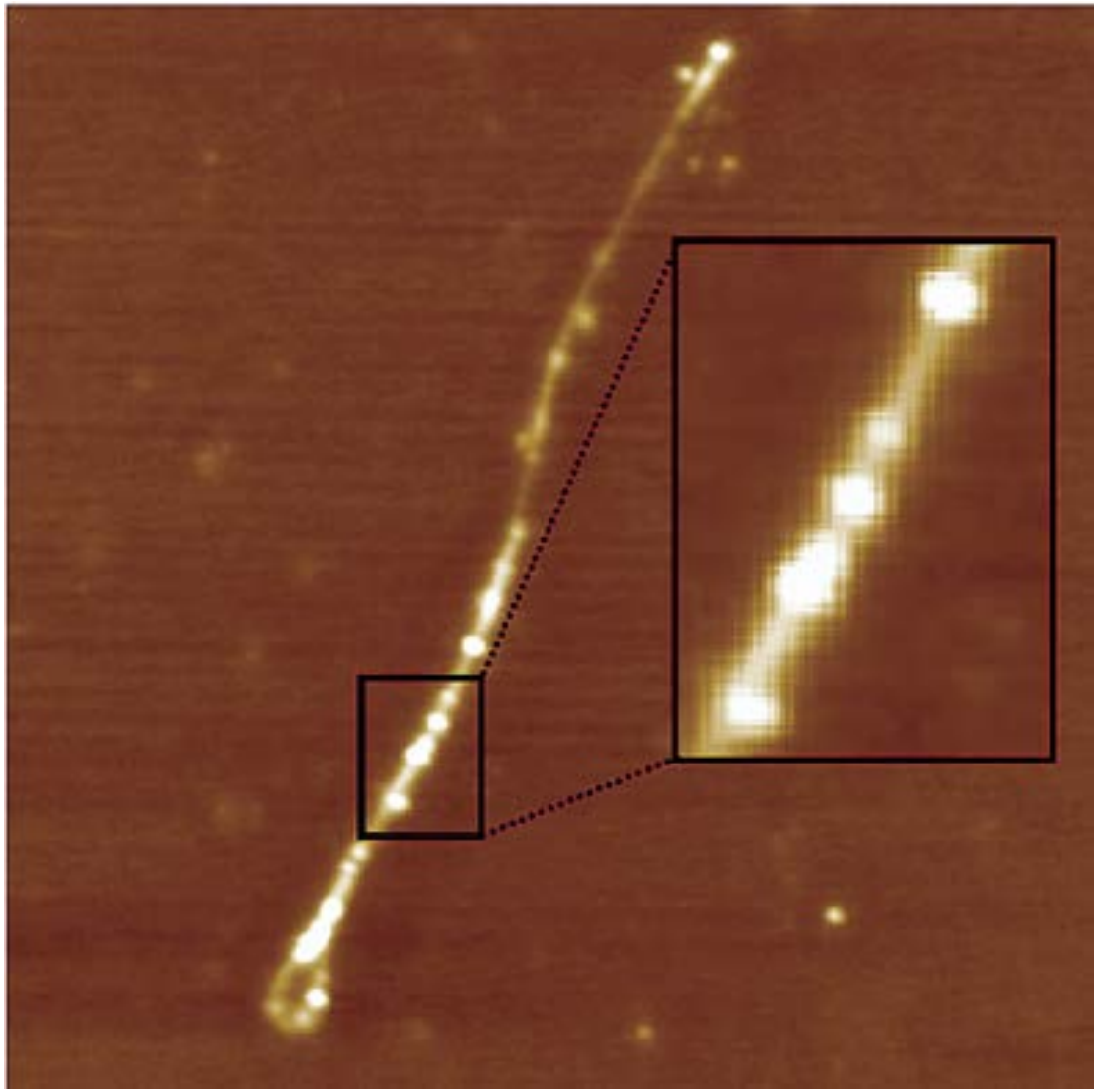

A typical tapping mode AFM (height) image of a SWNT functionalized by the Bingel reaction, [(COOCH2CH2SMe)2C<SWNT], and after exposure to ~5 nm Au colloids (4). The image shown is 900 nm × 900 nm, z scale 0–5 nm. The Au colloids can be seen (light colored features) decorating the complete length of the nanotube.

J. Am. Chem. Soc., 125 (29), 8722 –8723, 2003

Radical additions

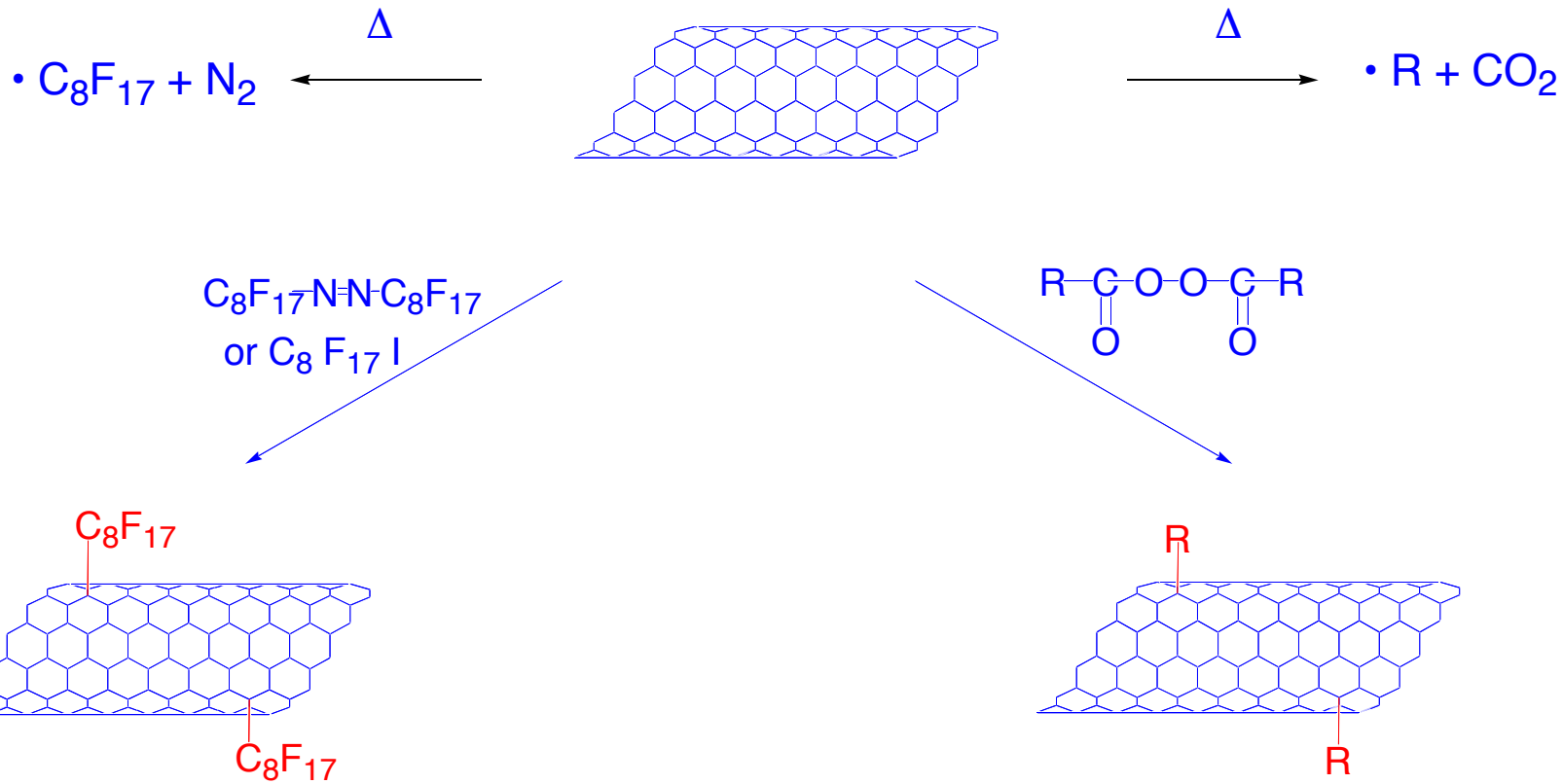

AC 2001 p4002, CC 2004 p1336

45 R = $-(CH_2)_{17}-CH_3$
46 R = $-(CH_2)_3-CH_3$
47 R = $-CH(CH_3)-CH_2-CH_3$
48 R = $-CH_2-CONH_2$
49 R = $-(CH_2)_3-Cl$
50 R = $-CH_2CN$
51 R = $-(CH_2)_3-OTHP$

CC 2003 p362, JACS 2003 p15174, OL 2003 p1471

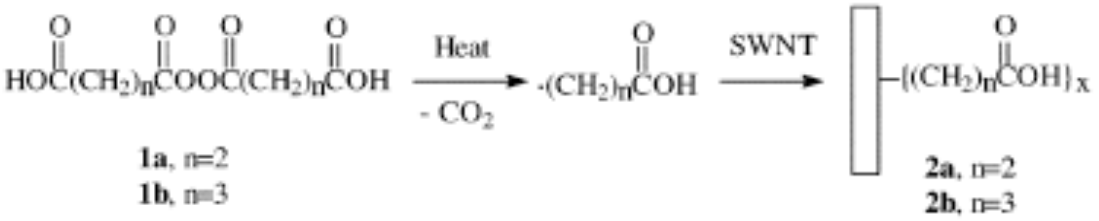

1a, n=2
1b, n=3

2a, n=2
2b, n=3

2a

SWNT-$CH_2CH_2CONHCH_2CH_2NH_2$

3

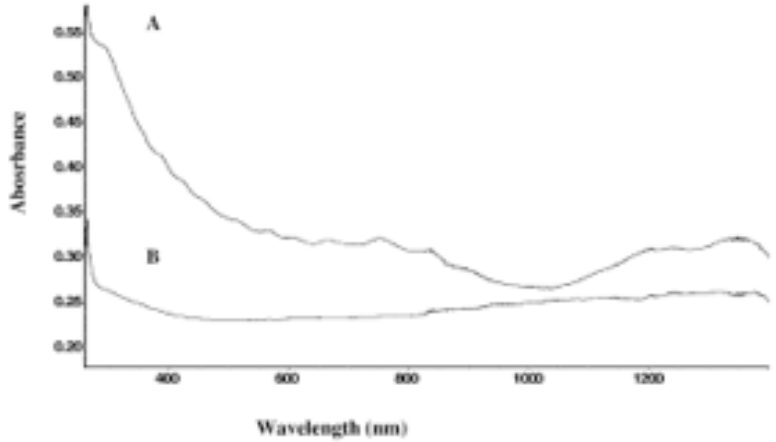

Figure 2. UV–vis–NIR spectra of (A) pristine SWNTs and (B) SWNT derivative 2a.

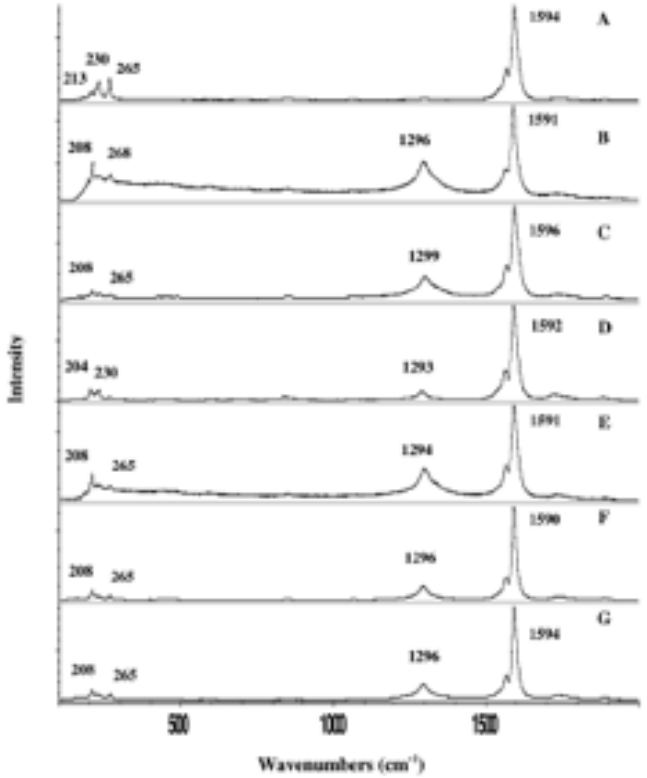

Figure 1. Raman spectra of SWNT materials: (A) pristine SWNTs, (B) 2a, (C) 2b, (D) SWNT residue after TGA of 2a, (E) 3, (F) 4, (G) 5.

Margrave, JL, Khabashesku, VN **J. AM. CHEM. SOC. 2003**, *125*, 15174–15182

Fluorination followed by displacement

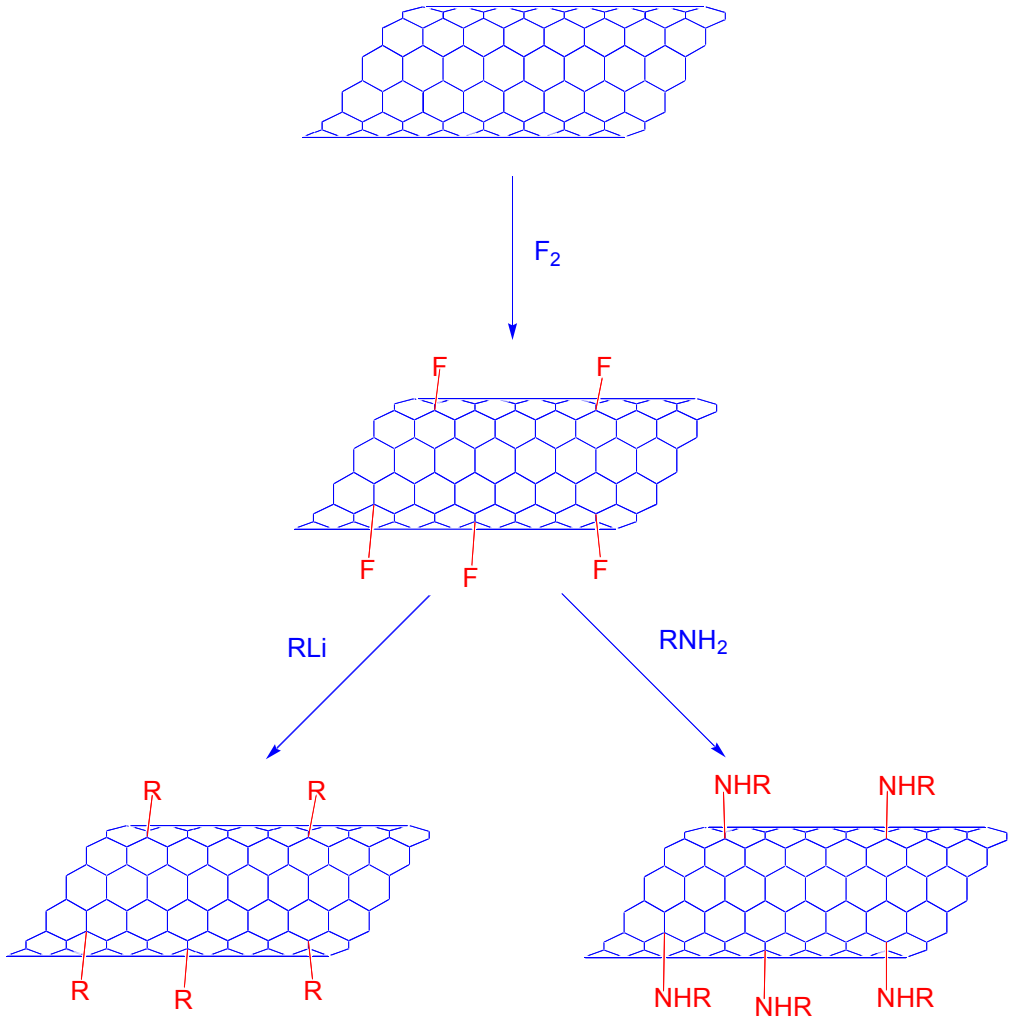

65 R = $-CH_3$
66 R = $-(CH_2)_3-CH_3$
67 R = $-(CH_2)_5-CH_3$

68 R = $-(CH_2)_2-NH_2$
69 R = $-(CH_2)_3-NH_2$
70 R = $-(CH_2)_4-NH_2$
71 R = $-(CH_2)_6-NH_2$

NL 2003 p 331, JACS 2003 p3617, CPL 1999 p367

Diazonium salts (Tour's approach)

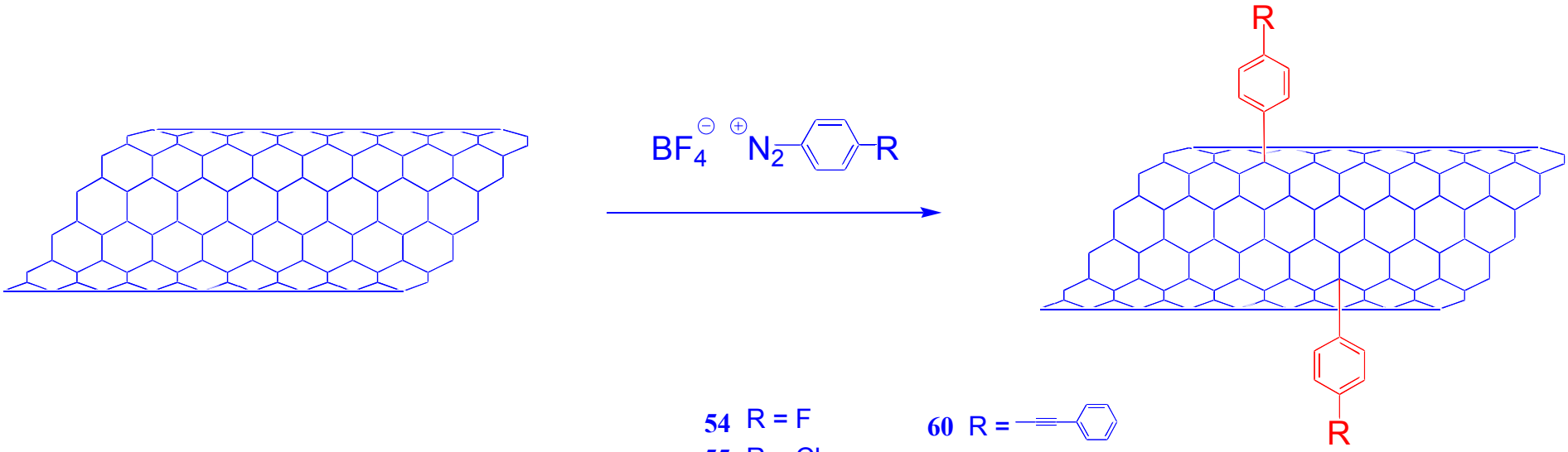

54 R = F
55 R = Cl
56 R = Br
57 R = *t*-Butyl
58 R = CO_2CH_3
59 R = NO_2

60 R =
61 R = $-C_{14}H_{29}$
62 R = 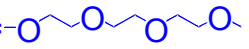
63 R = 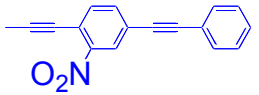

JACS 2001 p6536, Science 2003 p1519, NL 2003 p1215

Scheme 1. Functionalization of SWNTs Dispersed in Oleum[a]

1a, R = H, X = H to **1b**, R = SO_3H, X = H
2a, R = NO_2, X = H to **2b**, R = NO_2, X = SO_3H
3a, R = Cl, X = H to **3b**, R = Cl, X = SO_3H
4a, R = *t*-butyl, X = H to **4b**, R = *t*-butyl, X = H and SO_3H (~1:1)[b]
5a, R = CH_2CH_2OH, X = H to **5b**, R = CH_2CH_2OH, X = SO_3H[c]

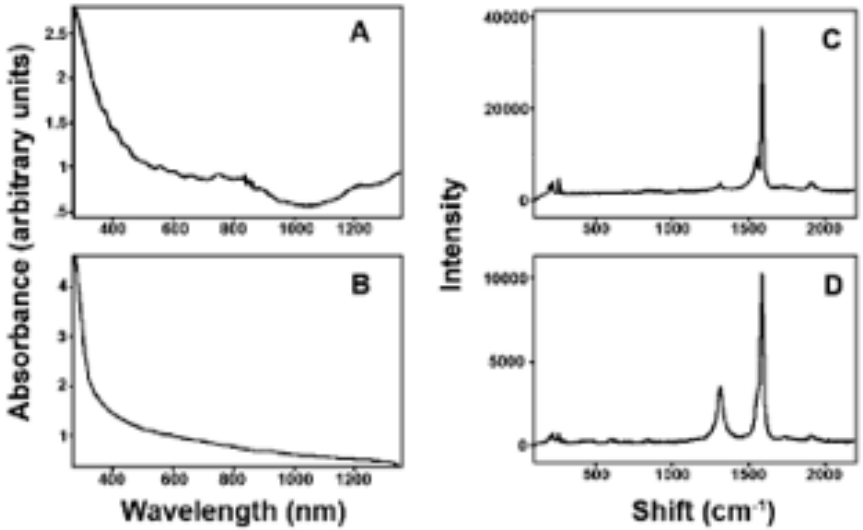

Figure 1. Absorption spectra of (a) p-SWNT in DMF. (b) **3b** in DMF. Raman spectra (solid, median scan of five different areas per sample, 633 nm) of (c) p-SWNT and (d) **3b**.

Tour, JM

Aligning Au Nanorods by Using Carbon Nanotubes as Templates

Luis M. Liz-Marzan et al. *ACIE* **2005**, *44*, 2.

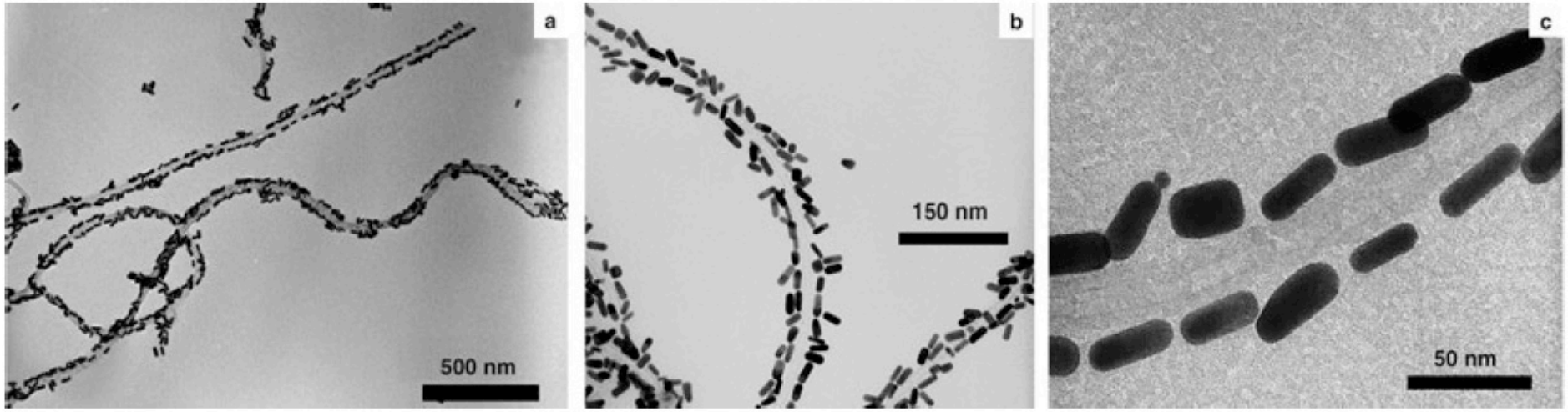

Figure 1. TEM images of Au nanorods (average aspect ratio 2.94), assembled on MWNTs (average diameter 30 nm) at various magnifications.

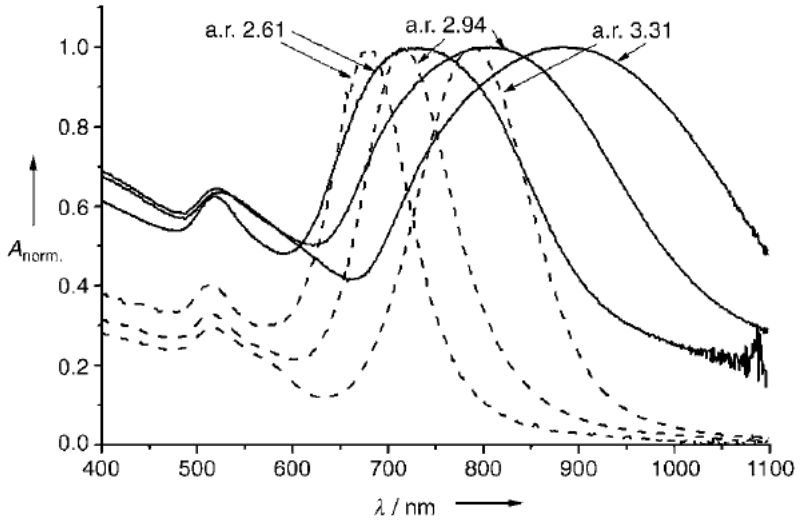

Figure 2. UV/Vis spectra of aqueous dispersions of individual Au nanorods (dashed lines) and nanorods attached on MWNTs (solid lines). The average aspect ratios (a.r.) of the nanorods are indicated.

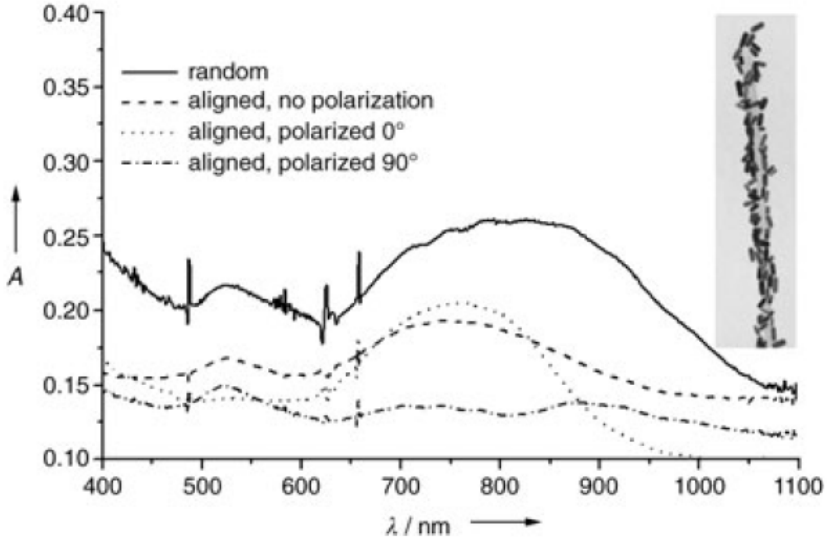

Figure 3. UV/Vis spectra of Au nanorod/MWNT nanocomposites dispersed in a PVA film before (-----) and after (——) stretching. Spectra of the stretched film using polarized light (•••••: 0°; –•–•: 90°) are also shown. The aspect ratio of the rods is 2.94. The inset shows a TEM image of a stretched Au/CNT composite in PVA.

CNTs characterization

TEM, SEM, AFM

TGA

RAMAN spectroscopy (can distinguish between metallic and semiconducting CNT, between pristine and functionalized CNT, but it fails to quantify the number of functional groups and their distribution)

radial breathing mode

Tangential modes

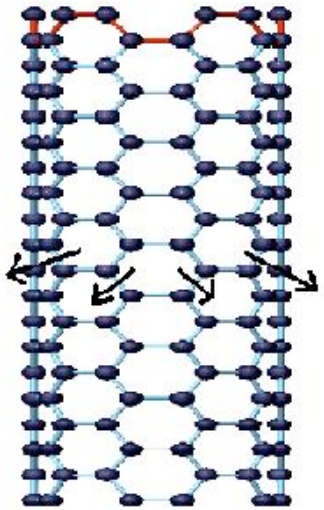

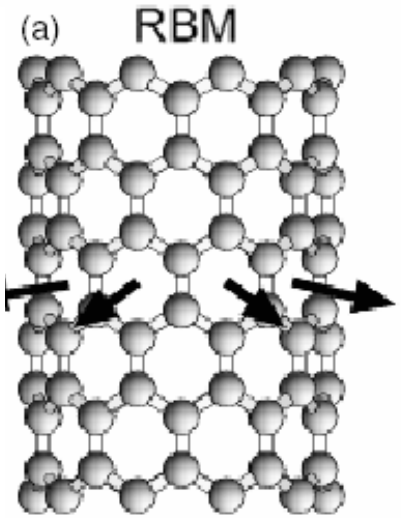

D-band: disorder-induced mode, indication of functionalization

120- 250 cm^{-1}

multi-peak features at 1580 cm^{-1}

The frequency of the RBM can be used to determine the diameter of the nanotube.
RBM mode, in fact, is proportional to the inverse of the nanotube diameter.
For CNT with d < 2 nm the G band is used.

HiPCO SWCNT

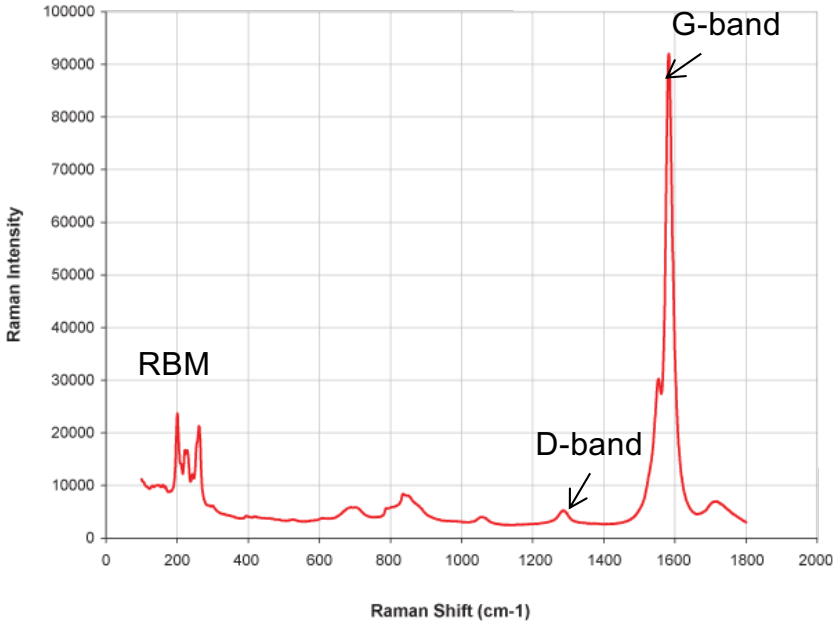

Raman spectrum of HiPCO SWCNTs using a laser wavelength of λexc = 633 nm.

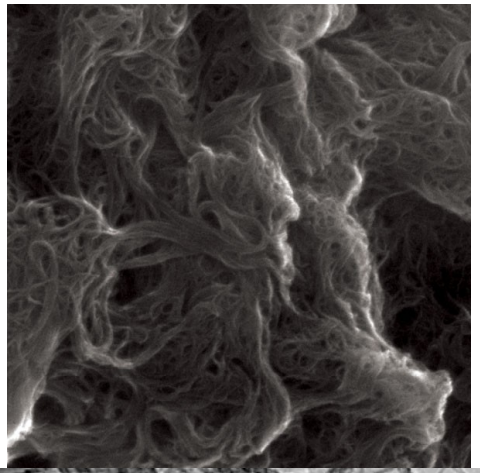

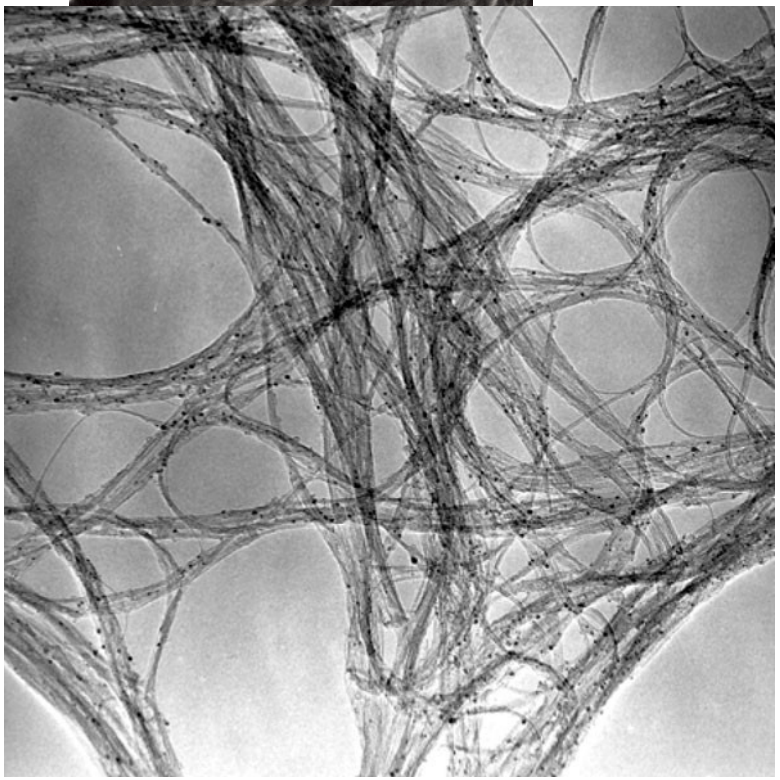

HiPCO – SWNTs produced by catalytic decomposition of carbon monoxide (HiPco-process)

Tangential modes (G-band)

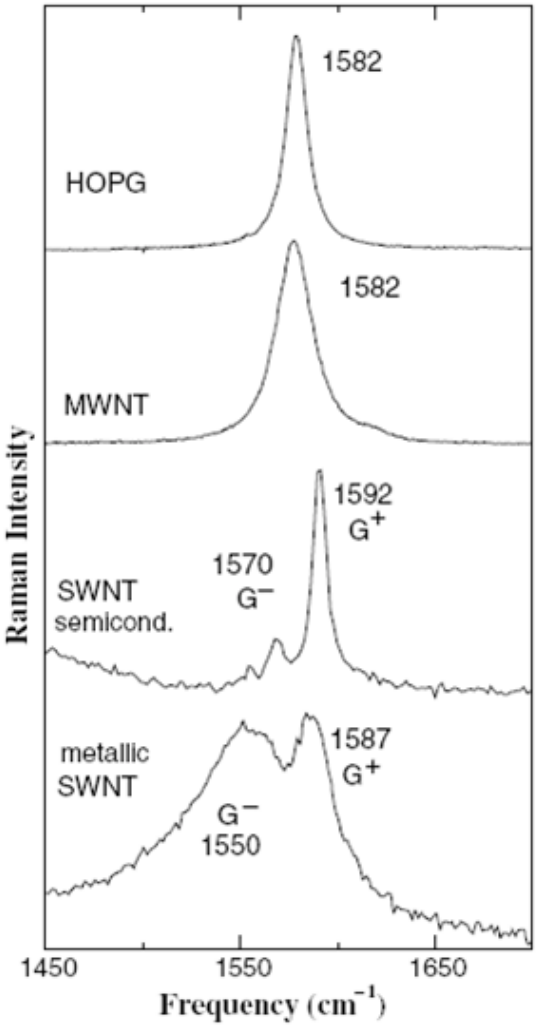

Schematic picture showing the atomic vibrations for the G-band.

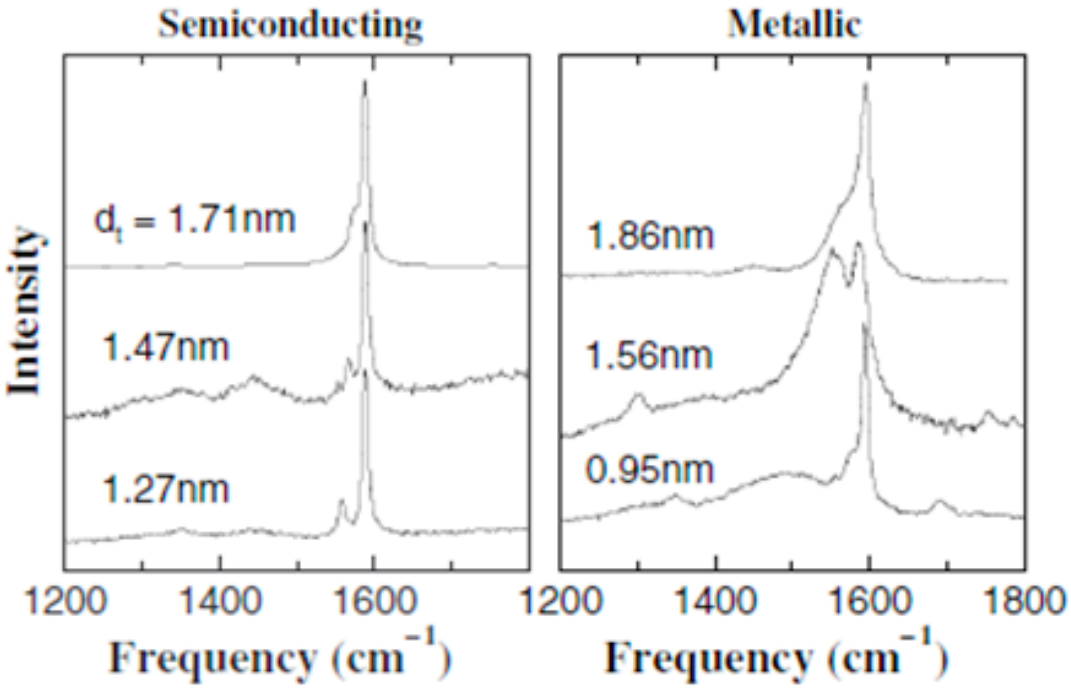

Raman signal from three isolated semiconducting and three isolated metallic SWNTs showing the G-and D-band profiles. SWNTs in good resonance (strong signal with low signal to noise ratio) show practically no D-band.

Single Wall Nano Horns

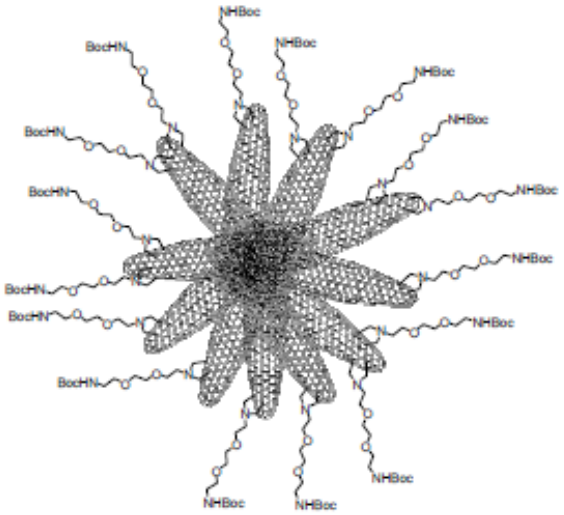

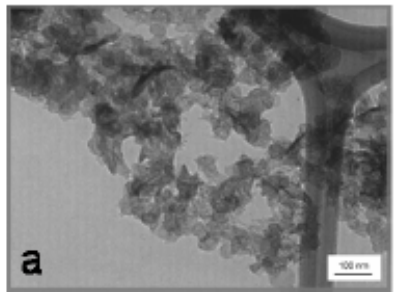

Carbon Nano Onions

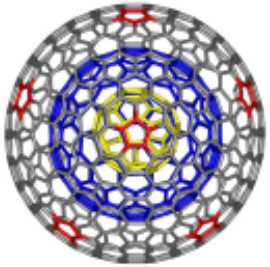

$C_{60}@C_{240}@C_{560}$

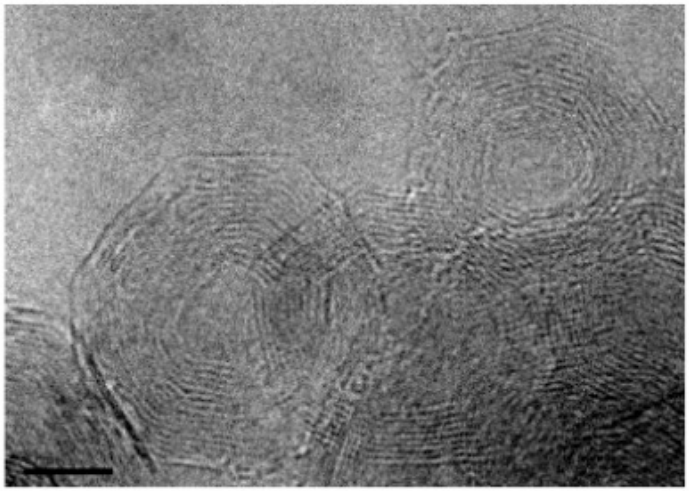

TEM picture of polyhedral CNOs.

CNT in biology and medicine

CNT present unique physicochemical properties such as electrical, thermal, and mechanical properties properties, high specific surface area, and capacity to cross biological barriers. These properties offer a variety of opportunities for applications in nanomedicine, such as
diagnosis,
disease treatment,
imaging,
and tissue engineering.

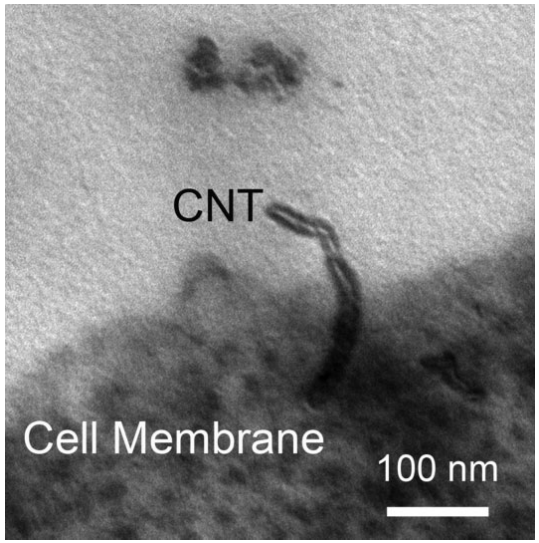

TEM of HeLa cells exposed to ammonium functionalized MWCNTs. CNTs successfully traverse the cell membrane, producing gene transfection.

Biocompatibility

nanomaterials may significantly alters the biological pathways
long term stability
biodistribution

Toxicity

Pristine CNT are toxic, their bewavior is similar to the of asbesto

many types of chemically **functionalised CNTs are biocompatible** with the biological milieu, highlighting how the *in vivo* behaviour of this material could be modulated by the degree and type of functionalisation, both critical aspects that need to be accurately controlled

Targeting carbon nanotubes against cancer

mechanism of internalisation (endocytosis or needle like penetration) is still not fully elucidated, it is generally recognised that CNTs are able to enter cells, inde- pendent of cell type and functional groups at their surface

- Delivery of chemotherapeutics: CNT–doxorubicin complexes

Treatments with 10 mg kg^{-1} of SWCNT–Dox (dose normalised on doxorubicin) instead of 5 mg kg^{-1} led to improved efficacy, without causing any severe toxicity.
Possible reasons are that the larger size of the SWCNT–Dox constructs, compared to free doxorubicin, probably slowed down the excretion rates and the PEG coating of SWCNTs could have hidden doxorubicin from macrophages.

CNTs have been shown to provide with:

(a) capability to deliver biologically active molecules cytoplasmatically, by-passing a lot of biological barriers and acting as a cellular needle;

(b) large surface area and internal cavity that can be decorated with targeting ligands and filled with therapeutic or diagnostic agents;

(c) unprecedented electrical and thermal conductivity properties

functionalization dramatically changes CNT properties, pharmacokinetic profile and, remarkably, even biodegradability

the resulting product properties will heavily depend on:
(1) the CNT material used (e.g. purity, diameter and length, number of walls);
(2) the PEG used (e.g. molecular weight, brush or mushroom conformation, branched or linear); and
(3) the functionalization process (e.g. level, surface density, homogeneity)

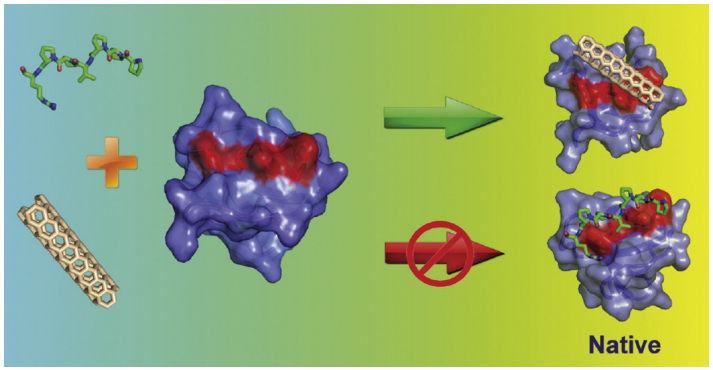

FIGURE 2

SWCNT and protein hydrophobic interaction. SWCNTs may fit into hydrophobic pockets onto proteins and interfere with natural ligand–protein interaction. Reprinted with permission from Ref. [58],

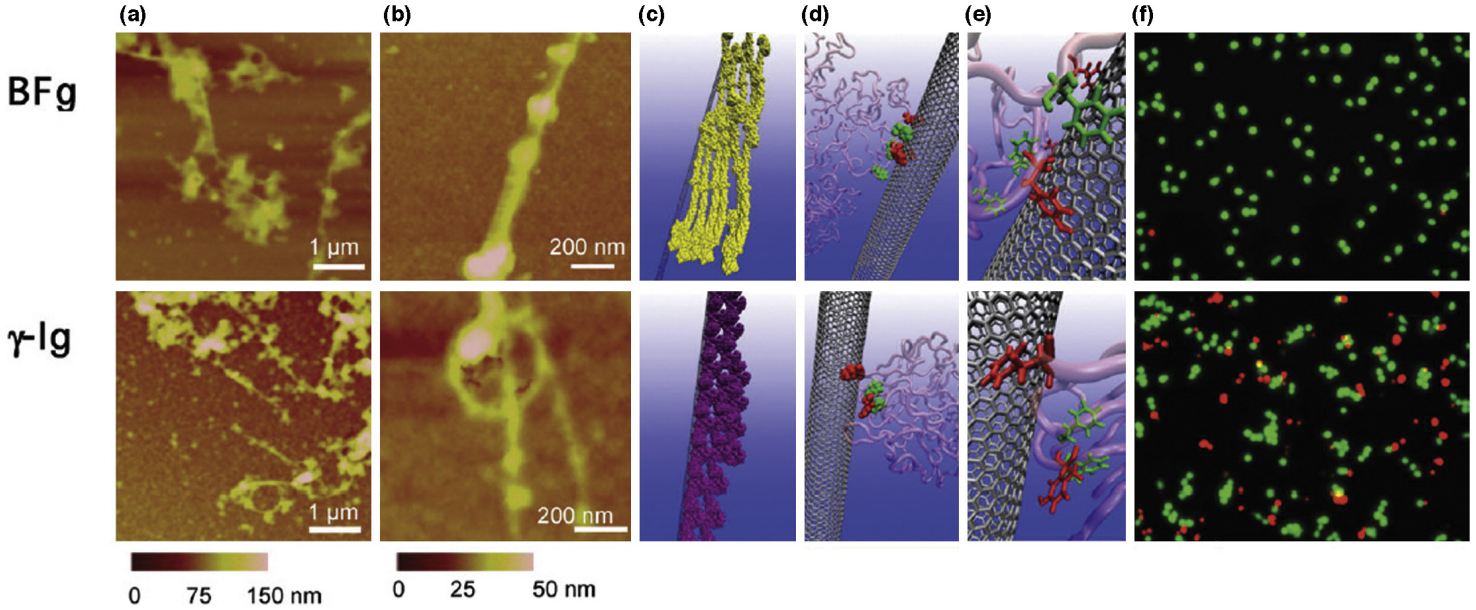

FIGURE 3

Interactions between two blood proteins (i.e. fibrinogen, BFg, *top*, and gamma-immunoglobulin, γ-Ig, *bottom*) and SWCNTs. AFM images of proteins after incubation with SWCNTs for 10 min (a) and 5 h (b). Molecular modeling illustrations for proteins (in beads representation) binding to SWCNTs after incubation for 10 min (c) and 5 h (d). (e) Locations of the most preferred binding sites for SWCNTs on proteins (pink cartoon, with highlighted tyrosine residues in red and phenylalanine residues in green). (f) The live (green) and dead (red) stains for THP-1 cells after treatment for 12 h shows reduced cytotoxicity for fibrinogen-bound CNTs (top). Reprinted with permission from Ref. [58], Copyright © 2013 Wiley-VCH.

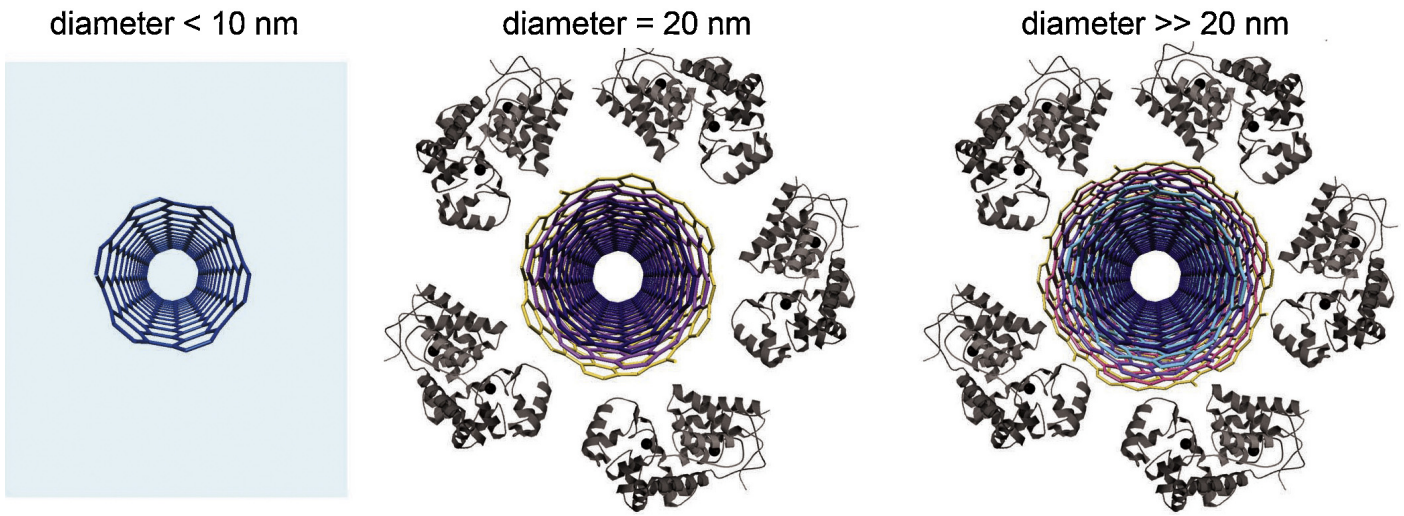

FIGURE 5

Formation of a protein corona around CNTs depends on the diameter of the tube. Nanotubes narrower than 10 nm (left) virtually bind no proteins on their surface, while for tubes with a diameter equal to or larger than 20 nm (center and right, respectively) formation of a protein corona is independent from the tubes width.

Immune system activation by CNT

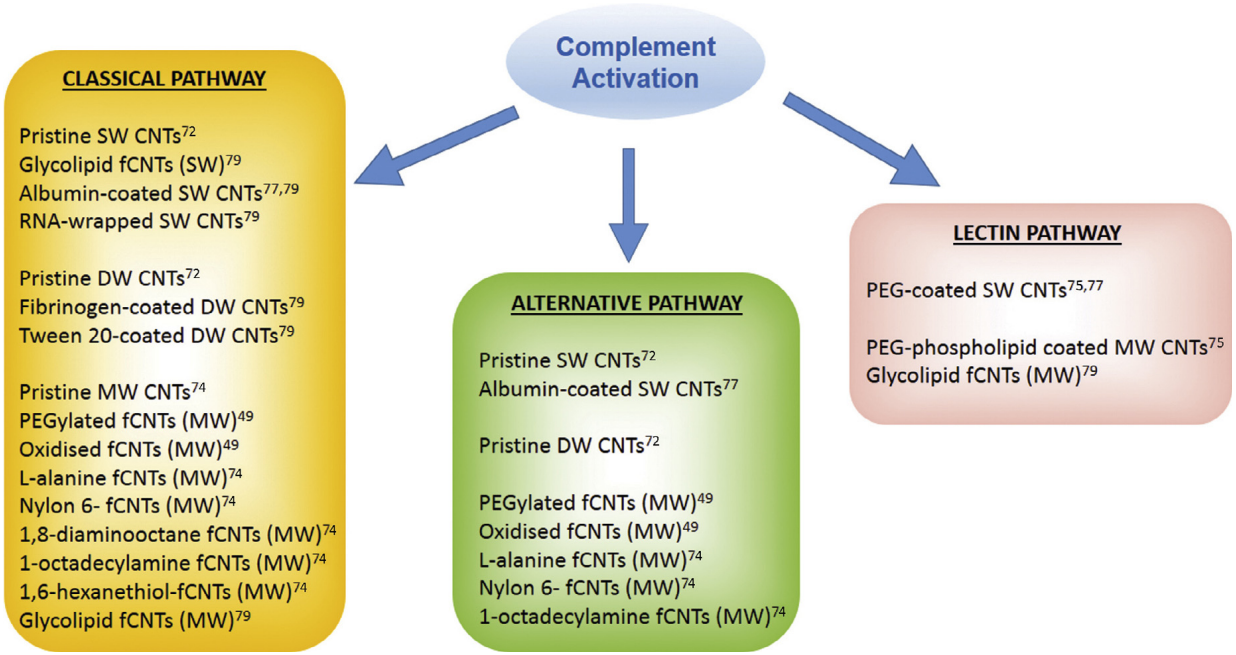

FIGURE 6

Functionalization affects complement activation pathway by CNTs. Several studies on *f*CNTs (single-walled, SW, double-walled, DW, or multi-walled, MW) reported on complement activation by CNT *via* classical (left), alternative (center), or lectin (right) pathways.

depending on the type and surface density of functional groups [48], and on the proteins that thus bind CNTs (e.g. immunoglobulins, complement proteins, or collectins)

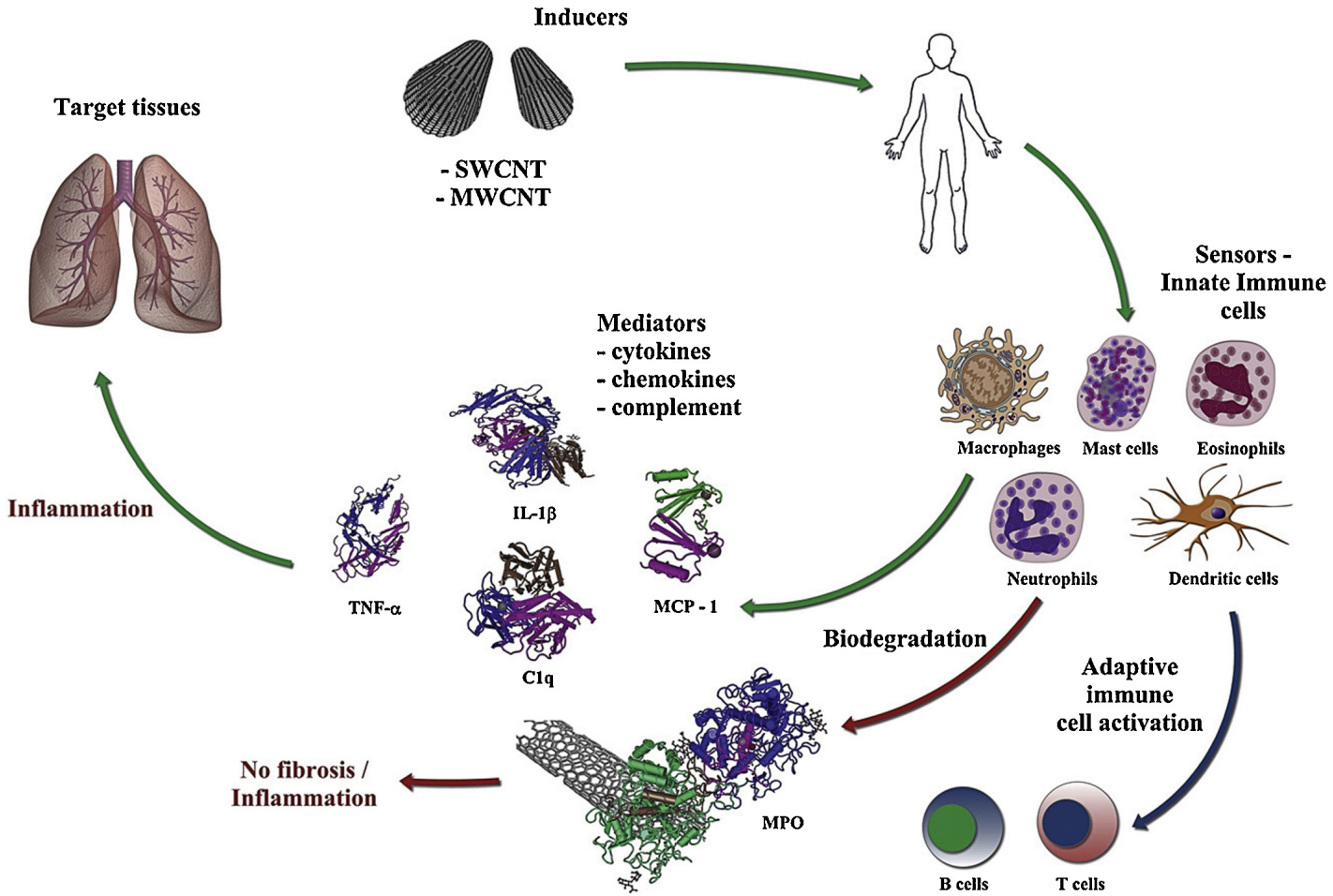

FIGURE 7

Immune response to CNTs. Three scenarios are possible: uncontrolled adverse inflammation (green pathway); biodegradation (red pathway); modulated immune response (blue pathway, e.g. for vaccine delivery). Reprinted from Ref. [36], Copyright (2013), with permission from Elsevier.

In culture, neurons and astrocytes grown on some CNT surfaces display reduced cell viability and adhesion, when compared to standard growth surfaces. However, one needs to be mindful of possible interference from the particles of catalyst and other admixtures which can account for a large part of toxicity observed in these studies. The presence of small amounts of soluble toxic components should also be considered.

CNTs may induce epigenetic changes that continue to exert effect long after CNTs are physically removed. This possibility is especially troubling because CNTs are extremely resistant to biodegradability, and may persist in the body indefinitely.

Immuno response by cells.

Carbon Nanotube Materials for Neural Electrodes

The extraordinary strength, toughness, electrical conductivity, and surface area of CNTs make them excellent candidates for interfacing with neural systems for the development of biocompatible, durable, and robust neuroprosthetic devices.

In 2000, it was suggested that CNTs could be used as substrates for neuronal growth. Scanning electron microscopy (SEM) was used to identify the morphological changes of neurons brought about by MWNTs. The neuronal bodies were found to adhere to the CNTsurface with neurites extending through the bed of CNT and elaborating into many branches. The neurons remained alive on the NTs for at least 11 days, and it was shown that several chemical manipulations on the MWNT enhanced neurites growth and branching. After this first report, several groups developed methods of neuron culture on CNT films.

NANO
LETTERS

2005
Vol. 5, No. 6
1107−1110

Carbon Nanotube Substrates Boost Neuronal Electrical Signaling

Viviana Lovat,[†] Davide Pantarotto,[†] Laura Lagostena,[†,‡] Barbara Cacciari,[§] Micaela Grandolfo,[||] Massimo Righi,[||] Giampiero Spalluto,[†,⊥] Maurizio Prato,*[,†,⊥] and Laura Ballerini*[,‡,||]

Scheme 1. Purification and Manipulation of MWNTs[a]

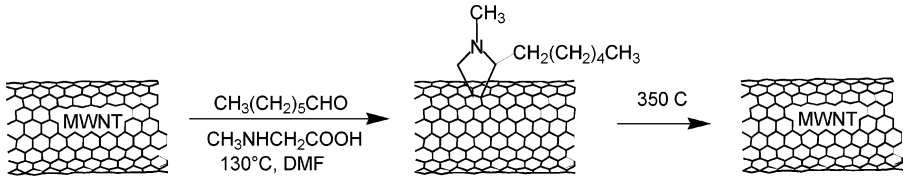

[a] The MWNTs were first functionalized and purified, then deposited on a glass substrate and heated to 350 °C, a process that eliminates the organic part, leaving intact the carbon network.

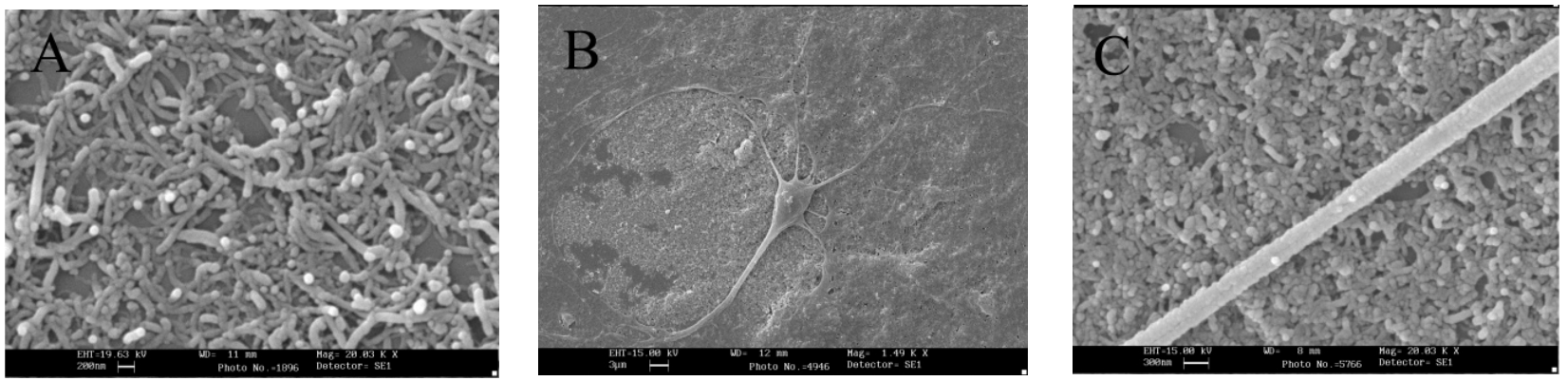

Purified multiwalled carbon nanotubes (MWNT) layered on glass are permissive substrates for neuron adhesion and survival. (A) Micrographs taken by the scanning electron microscope showing the retention on glass of MWNT films after an 8-day test in culturing conditions. (B) Neonatal hippocampal neuron growing on dispersed MWNT after 8 days in culture. The surface structure, composed of films of MWNT and peptide-free glass, allows neuron adhesion. Dendrites and axons extend across MWNT, glia cells, and glass. The relationship between dendrite and MWNT is very clear in the image in (C), were a neurite is traveling in close contact to carbon nanotubes.

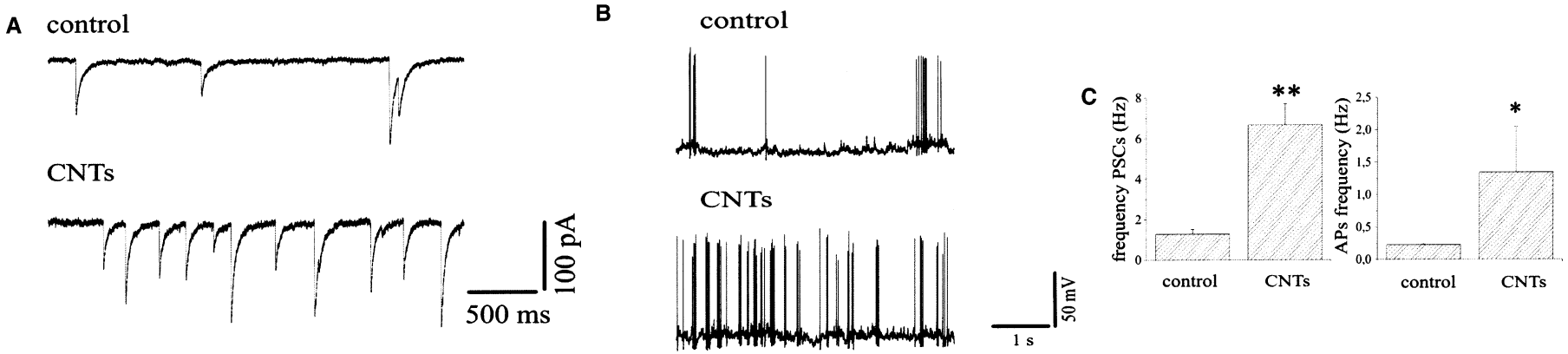

CNT substrate increases hippocampal neurons spontane- ous synaptic activity and firing.
(A) Spontaneous synaptic currents (PSCs) are shown in both control (top tracings) and in cultures grown on CNT substrate (bottom tracings). Note the increase in PSCs frequency under the latter condition. Recordings were taken after 8 days in culture. (B) Current clamp recordings from cultured hippocampal neurons in control (top tracings) and CNT growth conditions (bottom tracings). Spontaneous firing activity is greatly boosted in the presence of CNT substrates. (C) Histogram plots of PSCs- (left) and APs- (right) frequency in control and CNT cells; note the significant increase in the occurrence of both events when measured in CNT cultures. $^{**}P < 0.0001$ and $^{*}P < 0.05$.

The increase in the efficacy of neural signal transmission might be related to the specific properties of CNTs materials, such as the high electrical conductivity.

nature nanotechnology

ARTICLES

PUBLISHED ONLINE: 21 DECEMBER 2008 | DOI: 10.1038/NNANO.2008.374

Carbon nanotubes might improve neuronal performance by favouring electrical shortcuts

Giada Cellot[1], Emanuele Cilia[1†], Sara Cipollone[2], Vladimir Rancic[1], Antonella Sucapane[1], Silvia Giordani[2†], Luca Gambazzi[3], Henry Markram[3], Micaela Grandolfo[4], Denis Scaini[5], Fabrizio Gelain[6], Loredana Casalis[5], Maurizio Prato[2], Michele Giugliano[3,7‡] and Laura Ballerini[1‡*]

we show, using single-cell electrophysiology techniques, electron microscopy analysis and theoretical modelling, that nanotubes improve the responsiveness of neurons by forming tight contacts with the cell membranes that might favour electrical shortcuts between the proximal and distal compartments of the neuron.

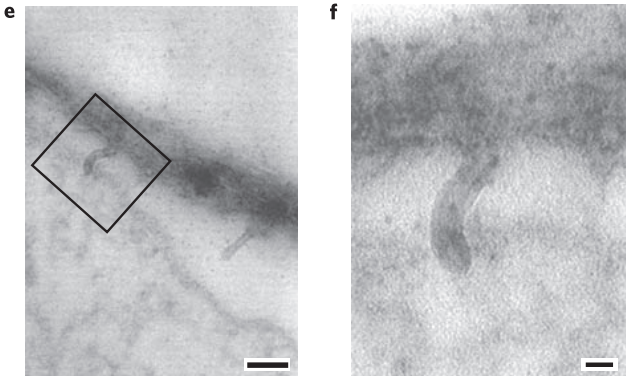

tight contact between nanotubes and membranes. The morphology of such contacts is indicative of the development of hybrid nanotubes – neuronal units .

High-magnification micrographs from a section consecutive to those of b and c. The rectangular area in e is magnified in f. Note how nanotubes are ‘pinching’ neuronal membranes.

nature chemistry

ARTICLES

PUBLISHED ONLINE: 8 AUGUST 2010 | DOI: 10.1038/NCHEM.761

Efficient water oxidation at carbon nanotube–polyoxometalate electrocatalytic interfaces

Francesca M. Toma[1,2], Andrea Sartorel[3], Matteo Iurlo[4], Mauro Carraro[3], Pietro Parisse[2,5], Chiara Maccato[3], Stefania Rapino[4], Benito Rodriguez Gonzalez[6], Heinz Amenitsch[7], Tatiana Da Ros[1], Loredana Casalis[2,5], Andrea Goldoni[5], Massimo Marcaccio[4], Gianfranco Scorrano[3], Giacinto Scoles[2], Francesco Paolucci[4], Maurizio Prato[1]* and Marcella Bonchio[3]*

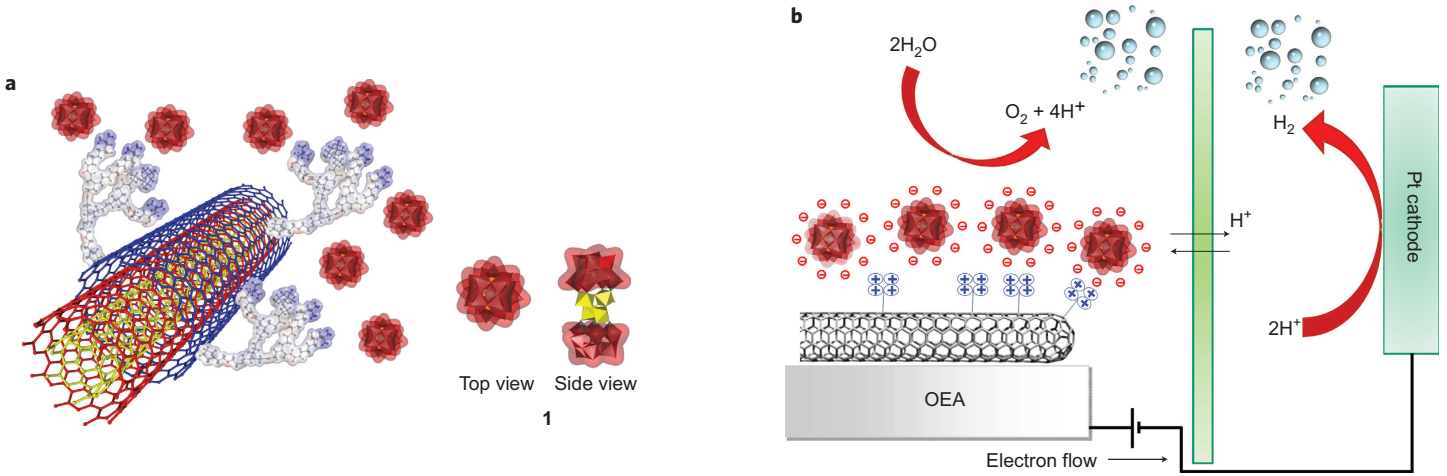

Figure 1 | Nanostructured oxygen-evolving material. a, Electrostatic capture of polyanionic ruthenium-containing clusters **1** (negatively charged, red surface) by polycationic dendrons on the MWCNT surface (positively charged, blue surface) and polyhedric structure showing the side and front view of the POM (red)-embedded tetraruthenate core of **1** (yellow). **b**, General scheme for a water-splitting electrocatalytic cell with the integrated nanostructured OEA.